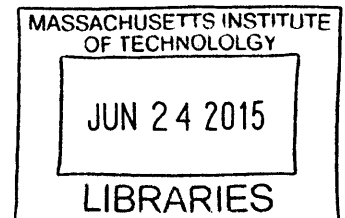


An Open Source Controlled Environment Agriculture Platform: Exploration of Root Zone Temperature Effects and Thermal Management

by
Camille Richman

Submitted to the
Department of Mechanical Engineering
in Partial Fulfillment of the Requirements for the Degree of
Bachelor of Science
at the
Massachusetts Institute of Technology
June 2015

ARCHIVES



© 2015 Massachusetts Institute of Technology
All rights reserved.

The author hereby grants to MIT permission to reproduce and to
distribute publicly paper and electronic copies of this thesis document in whole or in part
in any medium now known or hereafter created.

Signature redacted

Signature of Author.....

Department of Mechanical Engineering
May, 2015

Signature redacted

Certified by.....

Leon Glicksman
Professor of Building Technology and Mechanical Engineering
Thesis Supervisor

Signature redacted

Reviewed by.....

Caleb Harper
Research Scientist MIT Media Lab, Founder MIT CityFARM
Thesis Reader

Signature redacted

Accepted by.....

Anette Hosoi
Associate Professor of Mechanical Engineering
Undergraduate Officer

An Open Source Controlled Environment Agriculture Platform: Exploration of Root Zone Temperature Effects and Thermal Management

by
Camille Richman

Submitted to the Department of Mechanical Engineering
on May 20, 2015 in Partial Fulfillment of the
Requirements for the Degree of Bachelor of Science in
Mechanical Engineering

ABSTRACT

A first prototype of a GRObot open source controlled environment agriculture platform was built with air and water temperature control systems. Caesar basil seedlings were grown in the GRObot with a shallow water culture hydroponic system for two-week periods. In the first trial, the root zone temperature (RZT) was allowed to fluctuate with the air temperature resulting in an average RZT of 22.7°C, and in the second trial, the RZT was chilled to an average temperature of 20.5°C. For both trials, the air temperature was controlled to mimic a warm climate, with set temperatures of 30°C during the daytime and 25°C at night. The basil in the chilled RZT condition exhibited poor growth, while the basil in the fluctuating RZT condition exhibited the exponential growth expected of healthy seedlings. Temperature data recorded throughout these trials were used to construct a steady state thermal model of GRObot operation. Using this model, an interactive applet was created as a tool to help GRObot users predict electricity costs for environmental control with different environmental recipes to within two cents. This research demonstrates the first experiment aimed at determination of a crop's environmental recipe using the GRObot open source controlled environment platform.

Thesis Supervisor: Leon Glicksman

Title: Professor of Building Technology and Mechanical Engineering

Acknowledgements

The author would like to acknowledge Professor Leon Glicksman for his time and support in taking on this project as well as his advice and excellent mentorship both as a course professor and thesis advisor. The author would also like to thank Caleb Harper for taking her on as a researcher at the birth of the CityFARM project and for his mentorship over the past two years. Another thank you to the fellow undergraduate researchers of CityFARM who are such a fun bunch to work with, especially Emma Feshbach who also did her senior thesis on research in the development of open source controlled environment agriculture platforms. Thank you so much to Daniel Goodman, a primary research partner in building this first prototype of GRObot. Thank you also to Mike Sassoon for his dedicated mentorship and commitment to this research. Thank you to staff and students of the Ecological Greenhouse of Ein Shemer for continuously inspiring me and for providing space for the preliminary experiments of this study. Thank you also to Peter Konjoian for his willingness to provide feedback and discuss proper protocol for plant experiments. Thank you also to my family and friends who have brought me into this world, made this world beautiful, gotten me to MIT, and been a constant source of support. The author would like to extend a final thank you to the basil that gave their lives for this research.

Table of Contents

1. Introduction.....	6
1.1 Factors Necessitating New Food Production Methods.....	6
1.2 Feasibility of CEA and Soilless Farming.....	8
1.3 Solving a Shared Problem Together.....	13
1.4 GRObot’s First Challenge: Effects of Root Zone Chilling on Basil Growth.....	14
2. GRObot Build and Experimental Setup.....	17
2.1 GRObot Hardware.....	17
2.2 GRObot Control Systems.....	19
2.2.1 Lights and Air Temperature Control.....	19
2.2.2 Water Temperature Control.....	22
2.3 Root Zone Temperature Experiment Procedure.....	25
3. Thermal Characterization of GRObot.....	26
3.1 Determining Thermal Resistance Dictating Water Temperature.....	27
3.2 Calculating Energy Required for Reservoir Water Chilling.....	30
3.2.1 Energy Required for a System with Ideal Air Temperature Control.....	30
3.2.2 Energy Required for a System Based on Experimental Data.....	32
3.3 Interactive Applet: Calculating Energy Required for Environmental Control.....	33
3.4 Case Study: RZT Control for a Hydroponic System in a Greenhouse.....	39
4. Experimental Results.....	45
4.1 Effects of RZT on Basil Growth.....	45
4.2 Energy Consumption for Water Temperature Control.....	52
5. Future Work with GRObot.....	54
5.1 Hardware Developments.....	54
5.2 Networking Capability.....	55
5.3 The Community Approach to CEA.....	55
6. Conclusion.....	56
6.1 Building the First GRObot.....	56
6.2 RZT Effects on Basil Growth.....	57
6.3 Thermal Characterization of GRObot.....	58
Bibliography.....	59
Appendix.....	63

List of Figures

Figure 1-1: Types of hydroponic systems.....	7
Figure 1-2: Iterations of CityFARM prototypes.....	9
Figure 1-3: Hydroponic and aeroponic root growth.....	10
Figure 1-4: Sensing dashboards of the CityFARM web application.....	11
Figure 1-5: Dissolved oxygen versus temperature.....	15
Figure 2-1: GRObot structural frame and outer jacket.....	18
Figure 2-2: GRObot assembly with doors open.....	18
Figure 2-3: Hydroponic reservoir and plant tray setup.....	19
Figure 2-4: Light and air temperature control system schematic.....	20
Figure 2-5: GRObot temperature measurements without insulation.....	21
Figure 2-6: GRObot temperature measurements with insulation.....	21
Figure 2-7: GRObot shown with and without insulation.....	22
Figure 2-8: Water temperature control system schematic.....	23
Figure 2-9: GRObot temperature measurements with water temperature control.....	24
Figure 2-10: GRObot heat exchange system.....	24
Figure 2-11: Ebb and flow system.....	25
Figure 3-1: Thermal resistance network.....	27
Figure 3-2: Air and water temperature data for determining thermal resistance.....	28
Figure 3-3: Non-dimensional temperature versus time for determining thermal resistance.....	29
Figure 3-4: Idealized air and water temperature data.....	31
Figure 3-5: Chilling power required based on idealized air temperature data.....	31
Figure 3-6: Air and water temperature data with imperfect air temperature control.....	32
Figure 3-7: Chilling power required based on imperfect air temperature control data.....	33
Figure 3-8: Thermal resistance network overlaid on GRObot image.....	35
Figure 3-9: Applet home screen.....	36
Figure 3-10: Applet calculation based on parameters for RZT experiment.....	37
Figure 3-11: Applet drop-down list for jacket material selection.....	38
Figure 3-12: GRObot jacket wood customization.....	38
Figure 3-13: Experimental hydroponics setup in greenhouse.....	40
Figure 3-14: Greenhouse hydroponics setup air and water temperature data.....	41
Figure 3-15: Greenhouse solar irradiance data.....	41
Figure 3-16: Fish tank heater power usage.....	42
Figure 3-17: Greenhouse air temperature height stratification.....	43
Figure 3-18: Schematic of heat transfer modes on greenhouse hydroponic reservoir water.....	44
Figure 4-1: Basil fresh weight mass growth results.....	46
Figure 4-2: Basil stem height growth results.....	46
Figure 4-3: Dissolved oxygen at each RZT.....	48
Figure 4-4: Basil leaf and root appearance results.....	49
Figure 4-5: Water dynamic viscosity versus temperature.....	50
Figure 4-6: Peltier chiller watt metter data.....	52

1. Introduction

1.1 Factors Necessitating New Food Production Methods

Controlled environment agriculture (CEA) is gaining momentum as a sustainable augmentation to today's farming systems as the world's population booms, climate becomes more extreme, and resources become scarcer. By 2050, 9.6 billion people will share this planet, and 66% will live in cities.^{1,2} One hundred percent should have access to nutritious food. Because food production is not concentrated in cities, buying locally will be difficult, and the energy cost of moving food will grow. Eating will be harsher on the environment and the wallet.³ Extreme conditions associated with climate change such as floods and droughts will drastically effect production yields and consistency of supply.⁴ Shifting habitat ranges will disrupt food production systems and economies when temperate climate zones become tropical and tropical climate zones become superheated tropics.⁵ As temperatures rise, the space we grow crops in now will gradually be lost, and "today, 80% of the land suitable for growing food is already in use."^{6,7} Higher pressure on food production systems will require more freshwater. "Globally, the agricultural sector consumes about 70% of the planet's accessible freshwater."⁸ To move towards more sustainable farming practices is to move towards positive social and environmental change. Decreasing the prevalence of malnutrition, decreasing load on the planet's resources, and setting up systems that will ensure the health of the future population are all within the scope of scaling new, sustainable, CEA food production systems.

With CEA, production facilities can be placed anywhere, provide a higher level of protection from insects and disease, and be free from unpredictable and destructive weather events. Combine this with vertical farming, and production modules can be stacked to alleviate problems associated with space restrictions.⁶ Integration of hydroponic growing techniques with vertical farming can address space and water concerns. Most methods of hydroponics entail suspending plant roots in a fertilized water solution. Another growing technique, aeroponics, is a variation of hydroponics which has roots suspended mid-air and exposed to an atomized nutrient mist at a regular frequency. There are countless variations on these methods – recirculating versus drain-to-waste systems, variations in water depth, and high versus low-pressure aeroponics. Certain advantages to hydroponics and aeroponics include water and space conservation, controllability of

water content, and increased growth speed. Hydroponics and aeroponics can “cut water consumption by 90% compared to conventional agriculture” and “quadruple the growth speed.”⁷

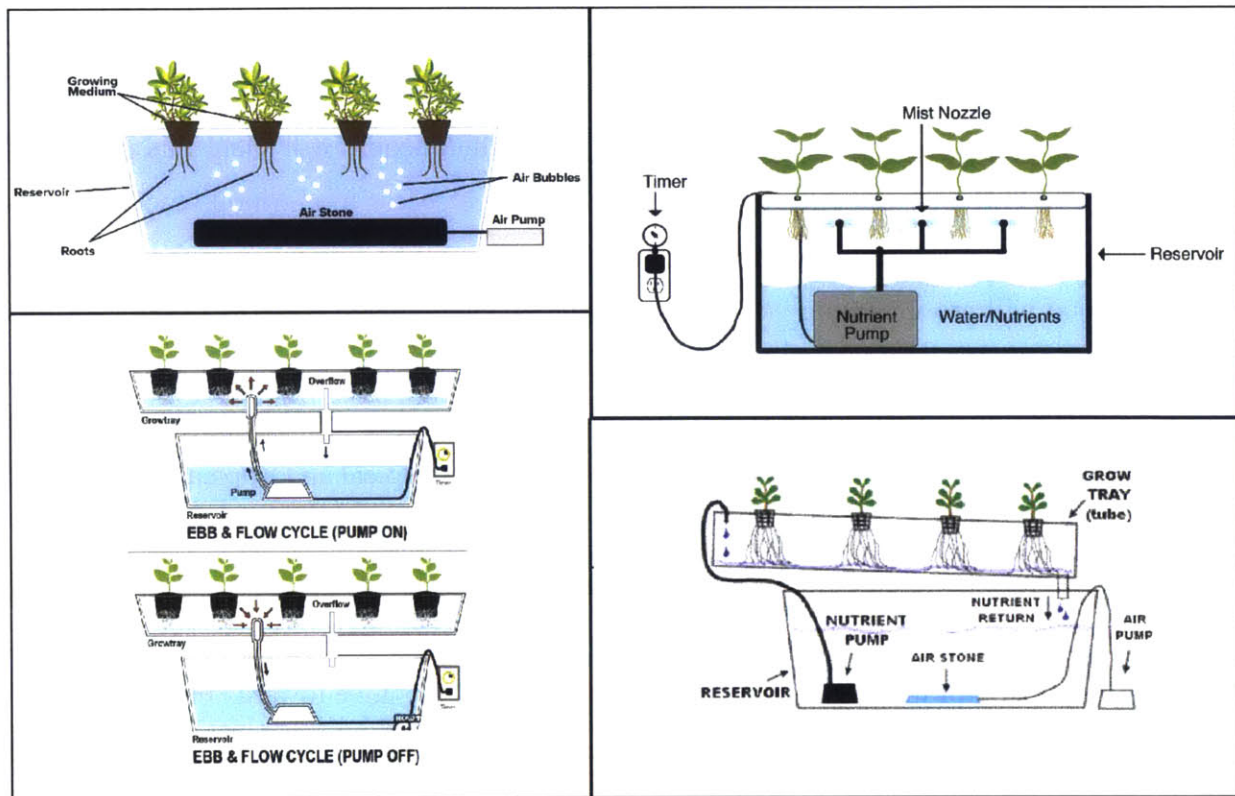


Figure 1-1: (Top Left) Deep water culture hydroponic system, in which roots hang in a reservoir of fertilized water aerated by an air pump and air stone.⁸ (Bottom Left) Ebb and flow hydroponic system, in which roots are exposed to fertilized water cyclically, with a timer dictating the frequency of ebb and flow.⁹ (Bottom Right) Nutrient film technique hydroponic system, in which roots are exposed to a thin flowing layer of fertilized, aerated water.¹⁰ (Top Right) Recirculating aeroponic system, in which roots are suspended in air and exposed to a nutrient mist at timed intervals.¹¹

CEA and soilless farming were born from attempts to grow food in extreme environments like outer space, Antarctica, and water-scarce regions. Hydroponics and aeroponics have been the subjects of proposals for many Lunar and Martian greenhouses, which could provide “water purification, oxygen production, various waste management tasks...and psychological benefits” for crew members.¹² NASA has conducted decades of research on soilless farming for microgravity environments and experimented with growing fresh food for crews on the Mir and International Space Stations.^{13, 14} At the Antarctic Casey, Davis, and Mawson stations, researchers outfitted insulated shipping containers with hydroponic farms to provide fresh produce

with limited amounts of water and avoid shipping potentially diseased plants to Antarctica, which is against environmental guidelines.¹⁵ As Earth faces the extremes in environment coming with climate change, moving towards scaling technologies that can provide operation uninhibited by outside influences while conserving water and space resources may be the necessary direction.

1.2 Feasibility of CEA and Soilless Farming

The CityFARM project at the MIT Media Lab has been studying feasibility and scalability of controlled environment soilless farming, having prototyped farms from the two-plant scale to the closet scale to the freight container scale. Each expansion has brought new labor and technological considerations to the table. The larger farms require more attention and organization, scaled sensing systems, and of course larger scale control systems. The team has expanded from one on the two-plant aeroponic system to six on the closet system to fifteen on the freight container size system. From daily maintenance and harvesting to sensor systems and website upkeep to prototyping next developments, the team is always busy. Throughout our operation of these hydroponic and aeroponic farms, we have succeeded in growing countless crops including tomatoes, lettuce, kale, broccoli, strawberries, peppers, beans, quinoa, radishes, basil, sage, dill, Swiss chard, cucumbers, and even cotton – to the point that we are confident in the methodology’s ability to grow nearly anything with a little experimentation on environmental parameters.

The current freight container sized farm, situated on the Media Lab’s façade, is monitored on five water sensing points: pH, dissolved oxygen, electrical conductivity, and temperature, and seven air sensing points: carbon dioxide, carbon monoxide, dust, humidity, temperature, and oxygen, and light intensity. These values are collected in real time and reported to the CityFARM website, which we can access from anywhere to check on conditions in the farm. Basic control systems exist for several parameters, however next steps for research include greatly enhancing the feedback capabilities of the farm. Now, fertilizer concentration and make-up are controlled by a system of passive Dosatron fertilizer injectors, water levels in reservoirs are triggered to automatically refill if too low, an air conditioning unit keeps temperature down during the heat of the day, and carbon dioxide is released from a pressurized tank to supplement atmospheric carbon dioxide. Feedback control on other sensing points, such as water temperature and air humidity, and improvement to and automation of current control loops are future research goals.

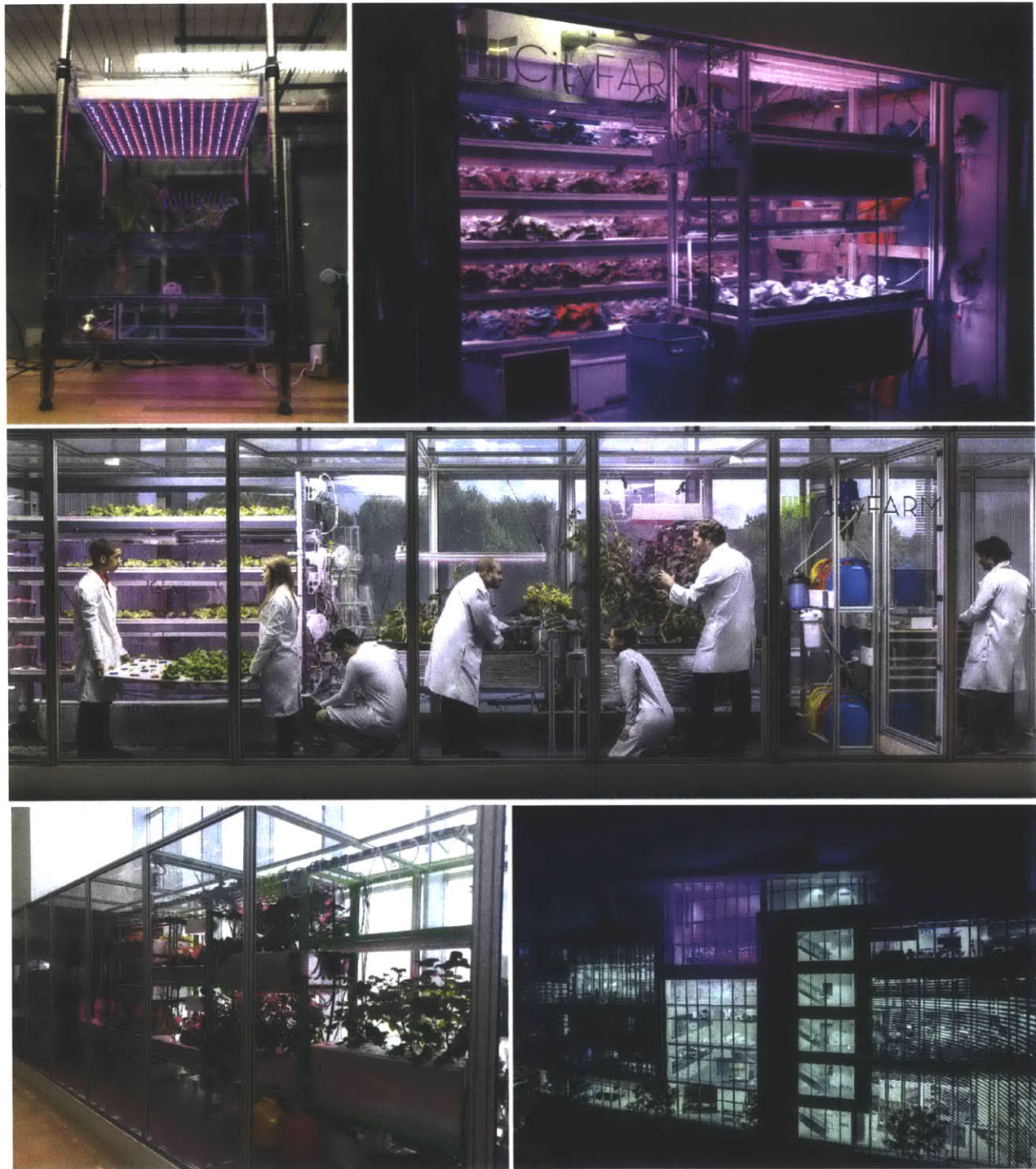


Figure 1-2: (Top Left) CityFARM's first prototype of an aeroponic system, growing two lettuce plants. (Top Right) Prototype of stacked hydroponic and aeroponic farms, situated in a closet space in the Media Lab. (Middle) Prototype built to experiment with hydroponics and aeroponics comprising a façade farm. (Bottom Left) Restructured façade farm. (Bottom Right) A view of the façade farm at night, with the purple glow of the LEDs emanating from the fifth floor of the Media Lab.



Figure 1-3: (Left) Roots of a royal burgundy bean plant growing in a shallow water culture hydroponic system. (Right) Roots of tomato plants grown aeroponically. Below the roots, the manifold that delivers the nutrient mist can be seen.

Air and water sensor data are continuously reported to the CityFARM website and logged to create histories of environmental conditions which can be crosschecked with plant and harvest dates. These histories create environmental recipes and can be referenced to match certain environmental conditions with phenotypic expressions, the observable characteristics, of the crops. With these tools, the effects of different environmental parameters on crop growth can be better understood and researched. It is these environmental recipes we are fine-tuning for various crop types and characteristics. With more developed control systems rigorous environmental recipe experimentation will be achievable, in which various sensing parameters can be strictly maintained while others are tested for effects on phenotypic expression. Through these recipes and open source hardware and software platforms, we aim to make CEA accessible to the masses through a grassroots at-home farming approach to scaling as well as through distribution of large scale farms for those interested in full-scale operation.

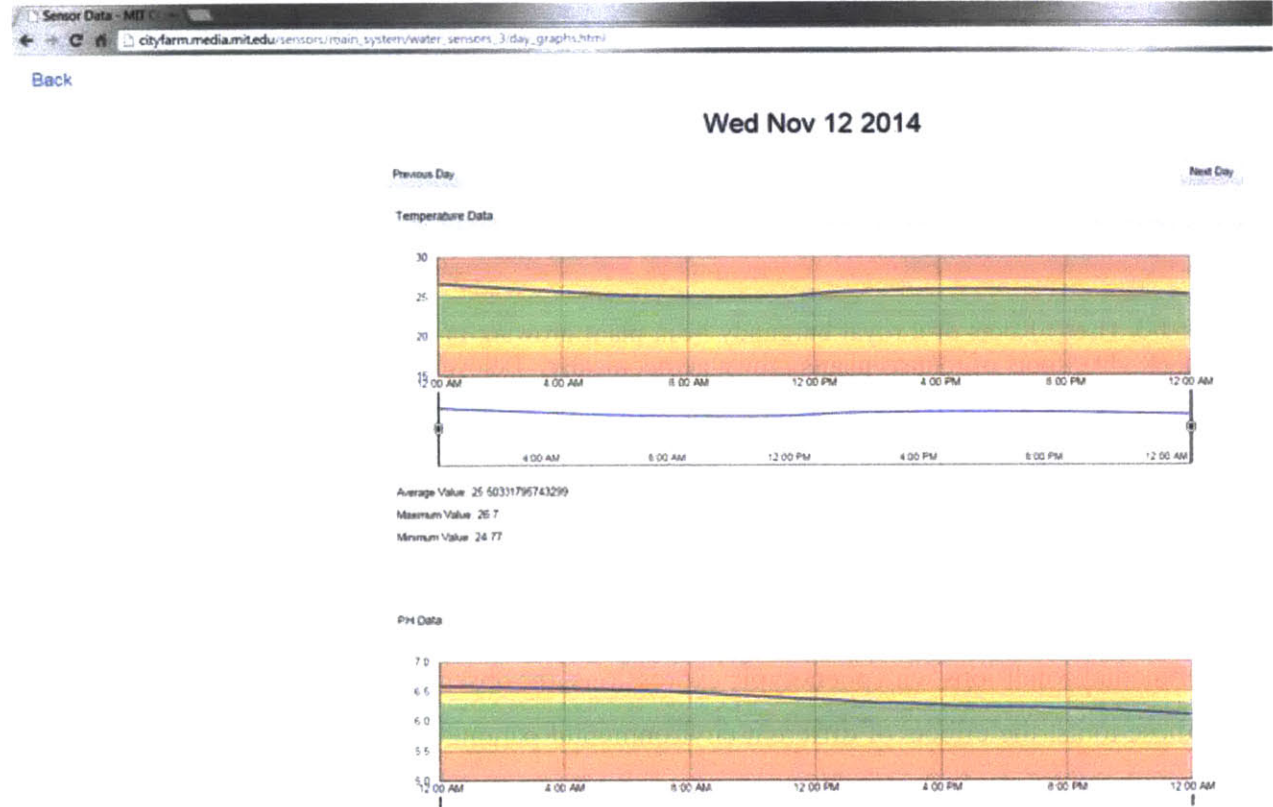
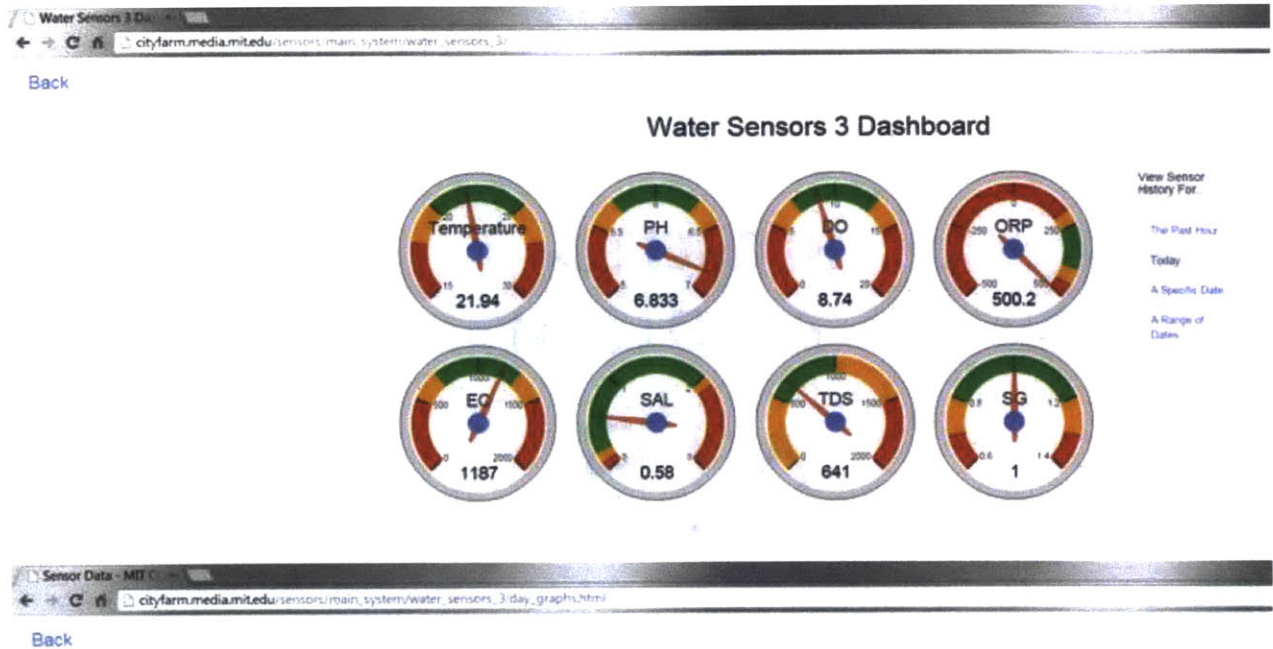


Figure 1-4: (Top) Sensing dashboard for hydroponic system number three in the façade farm, reporting temperature, pH, dissolved oxygen, oxidation reduction potential, electrical conductivity, salinity, total dissolved solids, and specific gravity. The dashboard updates in real time. (Bottom) Sensor data histories can be matched with the plant and harvest dates for crops to determine the environmental conditions in which the plant was raised.

When looking to these methods as sustainable options for food production, energy costs for artificial lighting, pumps, and environmental control systems must be considered. The main up-front and operational costs in vertical, controlled environment farms are for HVAC and supplemental lighting. Fluorescent, high-pressure sodium, and light emitting diode (LED) lighting are the most common choices, each with advantages and disadvantages pertaining to energy efficiency, capital cost, and spectrum control. Most growers are choosing artificial light over sunlight for access to high intensities of photosynthetically active radiation (PAR), light between 400 and 700 nanometers.¹⁶ The freedom yielded by LED panels is attractive to many growers in terms of spectrum tuning capabilities. Furthermore, LED technology is advancing faster than any other lighting technology: cost is decreasing and energy efficiency is increasing – an excellent trend for the viability of CEA and vertical farming having a large impact on food security.¹⁷ No matter how far advancements go, however, to implement controlled indoor farms will require significant energy for lighting and control systems, making renewable energy and efficient energy storage advancements a large player in feasibly scaling these systems. Farmers using space in office buildings may piggyback off of existing heating, ventilation, and air conditioning systems. Others may have to create environmental control systems from scratch. This brings advancements in energy efficient building design and research from greenhouse performance optimization to the forefront of the question of sustainability in new agriculture as well. With solar and geothermal energy options and intelligent building design, large production facilities could optimize their energy equations.¹⁸ Some research calculates that depending on availability of sunlight, size of solar panel array and battery storage devices, and specifications of heat exchangers, urban farms could theoretically achieve net zero energy usage or become net energy producers.¹⁹

Further affecting the feasibility of vertical CEA and its ability to meet a significant fraction of the required food supply is space. Where in crowded cities will these farms go? According to studies on unused space in cities, vacant lots are not hard to come by. Cleveland has 20,000 vacant lots; Philadelphia 30,900; New Orleans 14,000; and Chicago 70,000.^{20, 21} Urban CEA can help turn the problem of vacant lots into solutions that address urban food deserts and the growing population's nutritional requirements. Rather than a matter of space and technology, proliferating CEA in cities is a matter of public policy, public support, and public awareness. Many have recognized the potential of CEA and soilless farming methods as food solutions and pioneered research farms and production-scale vertical hydroponic farms. Such facilities exist in Japan,

Singapore, the Netherlands, Canada, and here in the United States in cities such as Detroit, Chicago, and Scranton, with plans for more in the works – for example in Jackson, Wyoming.^{22, 23, 24, 25, 26} Some of these vertical farms have failed due to complex design, high capital costs, or miscalculated energy costs, yet many are experiencing success and already distributing to local supermarkets.²⁷ These pioneering successes and failures are important but need to be interlinked for know-how and success to spread. For a crisis so huge – one facing the global population – a huge solution is needed, and people must be set up for success in running the sustainable farms that will feed our 2050 population of 9.6 billion. A solution will be one that requires cooperation and sharing, two words the current and burgeoning agricultural industries do not yet embody. A new agricultural system will require transparency for new farmers to be successful and subsequently, for all to be fed with a lighter impact on the environment.

1.3 Solving a Shared Problem Together

The CityFARM project is working to open up the industry via data sharing and creation of open source hardware and software platforms upon which anyone can build and share their findings through an online forum. With a standardized controlled environment farming platform, different researchers can work on the same experimental setup and have comparable data. Makers can design modifications to the platform to improve control systems and add new features. Farmers can explore with the platform to experiment with and transition into new agriculture methodologies in preparation for climate adaptation. Children can see these in their classrooms and grow their own food from an early age, gaining awareness about food technology. By the sharing of data – whether new environmental recipes, tutorials for building a new feature, or pictures of meals cooked from food grown in the environment – increasing transparency, increasing public awareness, and accelerating the advancement of CEA, vertical farming, and soilless farming can be achieved. It is the hope that through such an open source platform and community, the research and entrepreneurship that people are conducting separately now can instead be done jointly and more efficiently and garner more public involvement, advancing the technology to make an impact on global food security as soon as possible.

The CityFARM team is developing designs for three scales of this open platform: an at-home personal system called GRObot, a freight container size like the Media Lab façade farm called GROlab, and a warehouse-sized farm called GRObig. With these three systems all based

on similar standard chassis, sensor suites, and control systems, research done on any system will be adaptable to the others, and a community of growers and makers working at any scale can form a communal network of knowledge. Such a crowd-sourcing of research into CEA could help answer and solve crucial questions still lingering in the field. For example, five different light spectrums can be tested on the same crop in the exact same environmental conditions in people's GRObots located in five different countries. One hundred rice varieties can be tested in one hundred different GROlabs to determine which use the least amount of water when grown with various irrigation modules. GRObiggs can compete to produce the highest yield of or most nutritional crops with the least amount of energy and share their methods of energy consumption reduction. With so many parameters to test and optimize, crowd-sourced experimentation and fixes can answer important questions the public has about these technologies while simultaneously involving the public. As more awareness and credibility is garnered and more people have the tools to connect with their food, a more decentralized, transparent, stable, and sustainable agriculture system might begin to put a dent in supplementing or replacing current agricultural methods. This thesis explores the building of the first GRObot platform and the types of experiments users might conduct to explore CEA technology.

1.4 GRObot's First Challenge: Effects of Root Zone Chilling on Basil Growth

A root zone temperature (RZT) experiment was conducted in a GRObot to analyze the effects of chilling the water in a shallow water culture hydroponic system on basil growth. The technique of chilling RZTs has been used to trick temperate and subtropical plants to grow "all year round by cooling their roots while their aerial portions are subjected to hot fluctuating temperatures."²⁸ The technique has importance for those wishing to grow cooler climate crops like lettuce, broccoli, radishes, or spinach in greenhouses out of season or in tropical climates without unnecessarily spending energy on greenhouse air temperature control.²⁹ In the hobby hydroponics community, it is generally recommended that the RZT be several degrees cooler than the aerial temperature in order to give roots access to enough dissolved oxygen (DO) to allow root respiration.^{30, 31} Oxygen starvation can lead to poor water and nutrient uptake, increased susceptibility to pathogens, and wilting.³⁰ It is therefore recommended to introduce DO into hydroponic irrigation water to supplement levels of DO. Because saturation level of DO has an

inverse relationship to water temperature, water at colder temperatures can retain higher concentrations of DO.³²

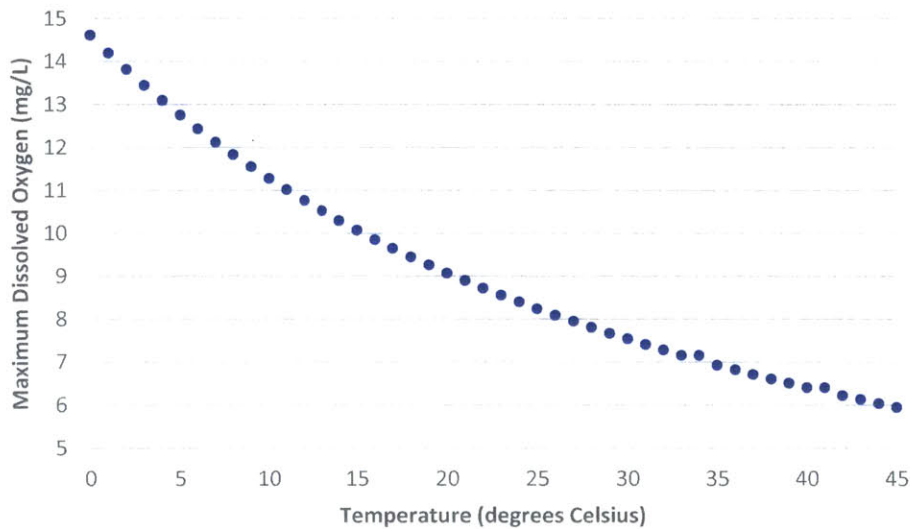


Figure 1-5: Oxygen solubility in freshwater as a function of temperature. Solubility decreases with increasing temperature.³²

Butter crunch lettuce, a cool climate crop, has been shown to grow well hydroponically at an air temperature of 31°C and root zone chilled to 24°C. The optimum set temperature for this crop appeared to be 24°C, with the higher and lower RZTs giving poorer crop yields. A cooler test case of 17°C water temperature and the warmer test case of 31°C water temperature yielded unfavorable results for dry mass yield as well as susceptibility to root disease. For all water temperatures tested, the DO was maintained at 8.4 mg/L.³³ This demonstrates that water temperature, independent of its relationship with DO concentration, has an effect on crop growth. Another study on hydroponic lettuce shows that increasing DO concentration at a constant water temperature can increase the rate of root respiration and that there is a threshold DO level of 1.4 mg/L below which lettuce roots do not respire.³⁴ However, another study found that DO levels in water at 24°C had no effect on lettuce growth, with measurements on fresh, shoot, and dry weights of lettuce grown at 2.1, 4.2, 8.4, and 16.8 mg/L of DO showing no significant difference.³⁵ These prior studies demonstrate that there are ranges of hydroponic RZT and DO conditions that can be suitable for lettuce growth.

Experimentally determining these ranges, with DO and RZT studied as both separate and linked parameters, is a worthwhile pursuit for research on all crop types. Varying these parameters may bring different taste, appearance, and other phenotypic expressions out in crops. Furthermore, knowledge of the ranges of all environmental parameters viable for growth of different crops can help spur the creation of environmental recipes suitable for multi-cropping. With a CEA system as big as the GROlab or GRObig, which might accommodate only one environmental recipe if not partitioned, a user will definitely want to grow many different crop types. This would require the meshing of each crops' environmental recipe. Knowing the acceptable ranges for each desired crop, an ideal recipe that accommodates all crops in the grow cycle can be constructed. Plants with larger ranges might be pushed to the extremities of their water temperature limits, for example, in order to accommodate a plant more sensitive to certain water temperatures. It may be that if no common ground exists between crops a user wishes to grow simultaneously in one chamber, separate smaller chillers could maintain separate RZT set points within the one growth chamber with distinct irrigation modules for each crop type.

This study is conducted to demonstrate a trial of a RZT chilling experiment conducted on basil, a warm climate crop. Basil and other warmer climate crops such as tomatoes and peppers are often eaten with cooler climate crops, which suits the assumption that farmers using the GROlab and GRObig systems will grow crops with very different environmental preferences at once. Will basil, being a warm climate crop, grow in the same chilled RZT conditions used to persuade temperate crops to grow with hot air temperatures? To find out, a GRObot was employed to simulate warm air temperatures, 30°C during the day and 25°C at night, to test basil growth at two different RZT conditions: (1) the water temperature was allowed to fluctuate with air temperatures and (2) the RZT was held at a constant 20°C. Testing with RZT of 20°C is based on findings that basil grown in NFT hydroponic systems with “prolonged exposure of the root zones to large amounts of warm (30°C) water was detrimental to root development,” the optimal RZT range for basil grown in tropical air conditions was between 25°C and 26°C, and the minimal RZT before observed root damage was 20°C.³⁶ The lowest viable RZT of 20°C was chosen for the first trial to initiate the determination of the viable range of the interlinked RZT and DO parameters for basil growth, beginning with the lowest RZT and therefore highest associated DO level. In the future, other RZTs in the 20°C to 30°C range and corresponding DO values will be tested.

2. GRObot Build and Experimental Setup

2.1 GRObot Hardware

A first prototype of the open source platform was designed, built, and subsequently used for basil root zone temperature experiments. GRObot measures 24 inches in length, 19 inches in depth, and 30 inches in height. The chassis is constructed of 80/20 aluminum extrusions and standard 80/20 bracket attachments. The chassis is enclosed by a ¼” acrylic jacket with hinged doors on all sides but the back. Windows were laser cut and covered with opaque green ¼” acrylic. Delta 12038 240 CFM computer fans are mounted to the laser cut top door vents, pulling air through the side door vents. A 200W Lasko #100 MyHeat Personal Heater sits in the back left corner of the system, above the 1” thick Styrofoam plant tray floating in the Sterilite 28-quart reservoir and below the two Lvjing 120W 1365 LED Plant Grow Light Panels.

A Sterilite 28-quart storage box sits on the base of the chassis as the hydroponic reservoir, holding the nutrient water, air stones, and small aquarium pump that comprise the shallow water culture hydroponic irrigation system. JRPeters Nitrogen-Phosphorous-Potassium fertilizer is mixed into the water for an electrical conductivity of 1.2 and a pH of 6. 16-4-17, 5-12-26, and 0-0-15 fertilizers were mixed at a 1:2:1 ratio with a concentration of approximately 1.2 g/L. An EcoPlus 728450 air pump pushes air from outside GRObot through three air stones to saturate the water with dissolved oxygen. A PP09205 92 GPH submersible aquarium pump circulates water within the reservoir, allowing for increased oxygenation and nutrient movement. The 1” Styrofoam tray with 35 1” square holes floats atop the nutrient water, holding the plants in place with roots in the water and leaves emerging above the tray.

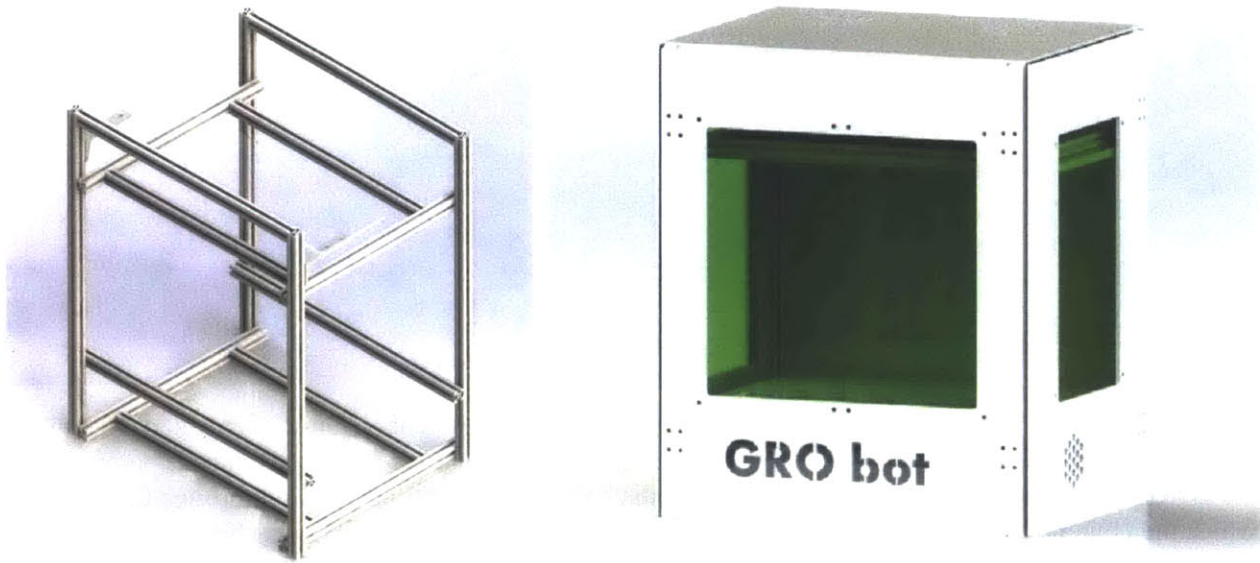


Figure 2-1: (Left) Render of GRObot chassis constructed with 1" 80/20 extrusions. A bottom shelf holds the hydroponic reservoir, while the top shelf supports the grow lights. Above the upper 80/20 shelf is a clear acrylic sheet which holds the electronics for the control systems. (Right) Render of GRObot with its acrylic outer jacket.

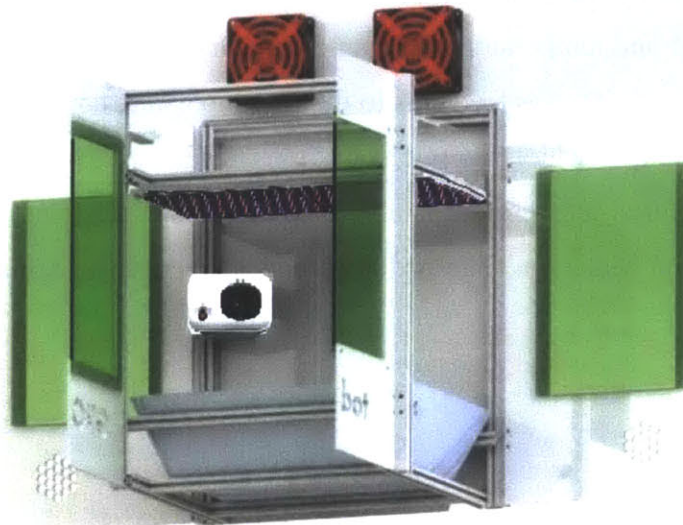


Figure 2-2: Render of GRObot with all doors open. Hydroponic reservoir sits at base, with heater placed above in back corner and red/blue LED panel illuminating from top shelf. Two fans are mounted to top door, pulling air through hexagonal vents on side doors.

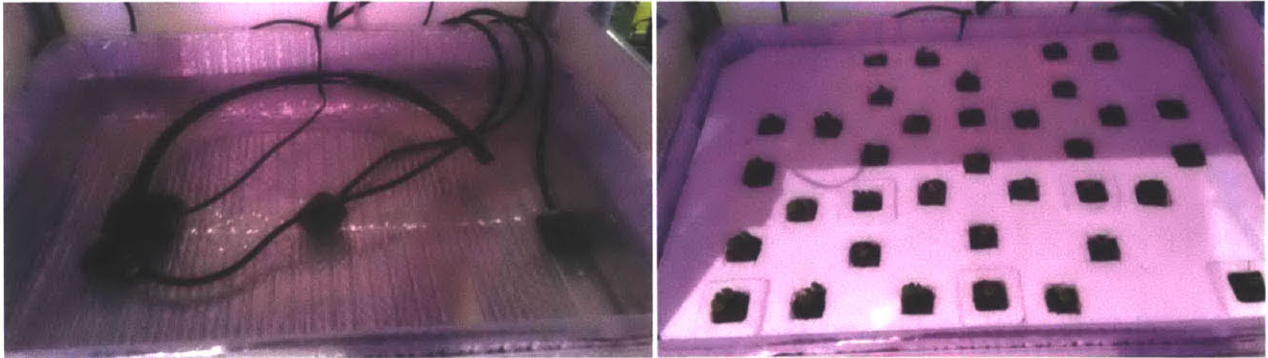


Figure 2-3: (Left) The hydroponic reservoir internal setup. The submersible pump and 18” tubing attachment create flow within the reservoir water. The three air stones are attached to an air pump outside the system, which pulls in air from the ambient Media Lab environment and pumps it through the air stones which then bubble the air into the water. (Right) The 1” thick Styrofoam tray floats above this setup, with 35 1” square cutouts for the plants to sit in. The plants are held in place by Horticulture foam substrates.

2.2 GRObot Control Systems

2.2.1 Lights and Air Temperature Control

During daytime hours, declared to be 06:00 to 24:00, LED panels turn on and the air set point temperature is defined as 30°C. During nighttime hours, LED panels are turned off and the air temperature is set to maintain 25°C. A SainSmart real time clock module reports the hour to an Arduino Uno microcontroller, which ascertains whether it is daytime or nighttime and executes the corresponding light and temperature commands. A Grove DS18B20 temperature probe rests on the Styrofoam tray and serves as feedback to the air temperature control loop. A simple control system was implemented, in which the microcontroller reads the temperature every 20 seconds, determines if the measured temperature is above or below the set point, and turns fans on and heater off or fans off and heater on. The Arduino code is given in the Appendix.

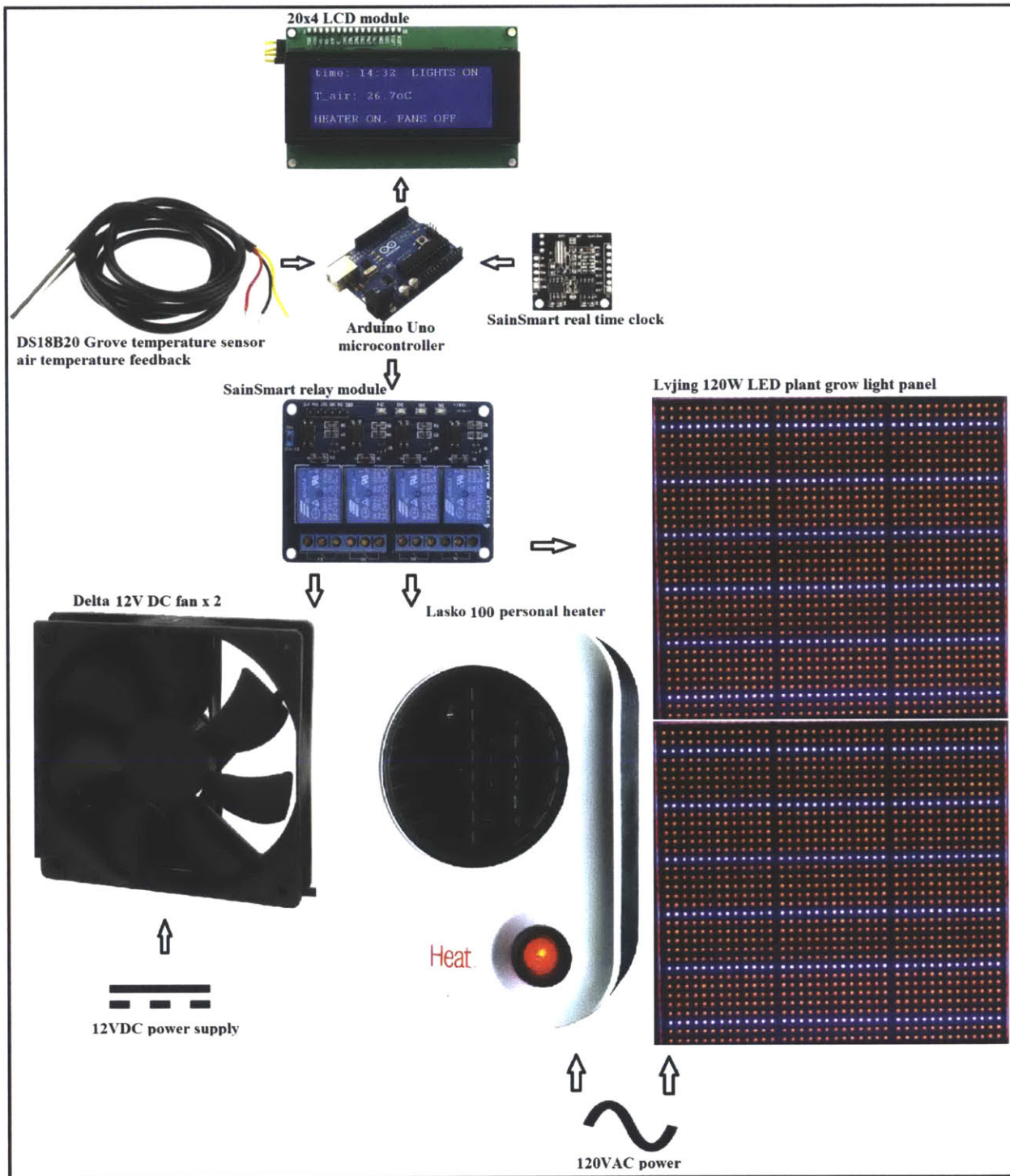


Figure 2-4: Schematic of light and air temperature control system. The microcontroller takes time and air temperature as input and accordingly switches certain components on through the relay module. The time, temperature, and status of components are displayed to the user on the LCD.

Upon first implementation of the air temperature control system, it was found that thermal insulation improvements to the GRObot outer jacket were necessary. Gaps in the acrylic and the low thermal resistance of acrylic at 0.2 W/mK proved to make air temperature control difficult.¹⁵ The set point temperatures were rarely reached or maintained, as the heat leaking to the outside rendered the air temperature control system inadequate. To make the control system more effective, 0.3125” thick Reflectix radiant barrier insulation was installed to cover gaps and layer against the acrylic back, side doors, and parts of the front door. The Reflectix has the added benefit of decreasing LED light leakage through the windows and white acrylic.

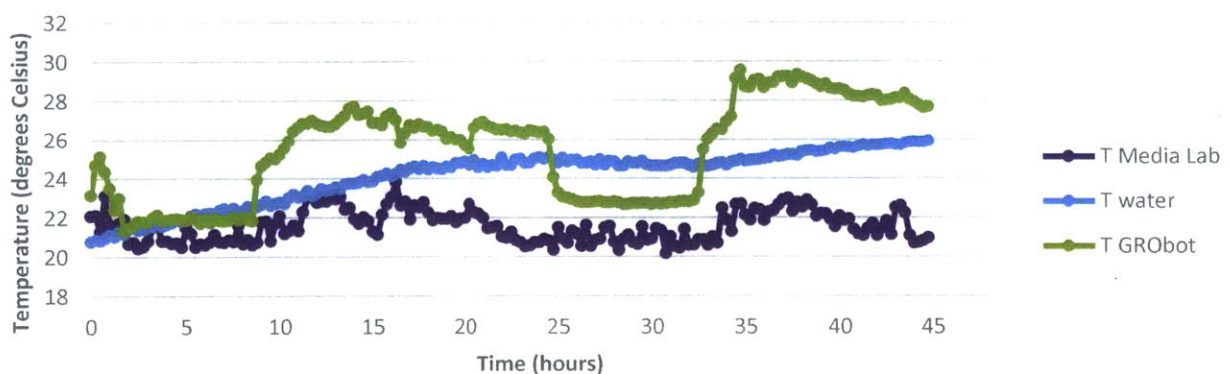


Figure 2-5: Temperature measurements of the Media Lab 5th floor CityFARM space, air inside GRObot at the Styrofoam tray, and water in the hydroponic reservoir. The targets of 30°C during the day and 25°C at night are not met without the added Reflectix insulation.

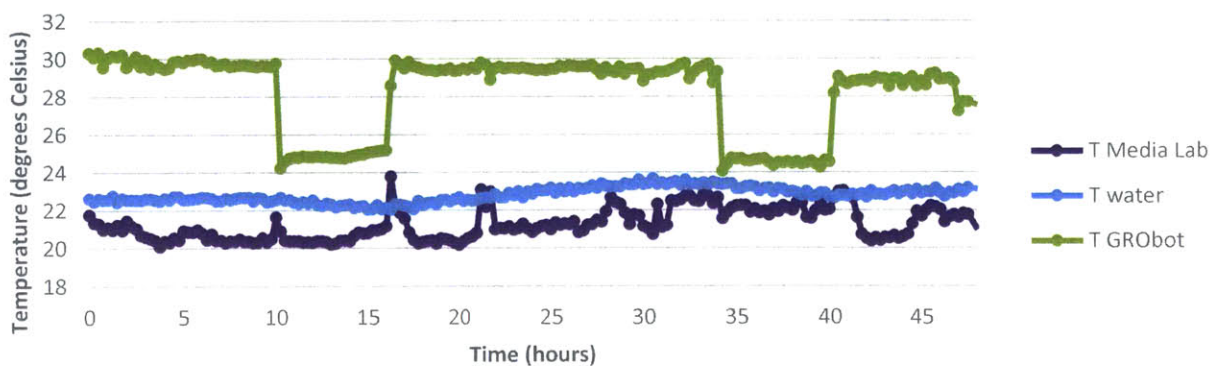


Figure 2-6: Temperature measurements of the Media Lab 5th floor CityFARM space, air inside GRObot at the Styrofoam tray, and water in the hydroponic reservoir. With the Reflectix insulation used as an additional layer against the acrylic jacket, the air temperature control system is able to maintain the set temperatures more effectively.

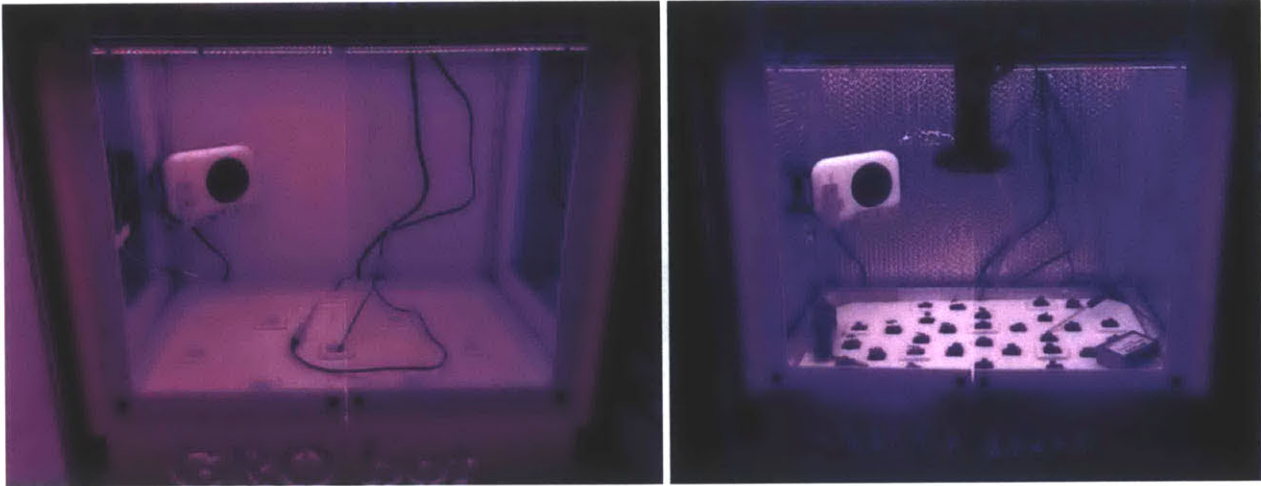


Figure 2-7: (Left) GRObot shown without added insulation. Light and thermal leakage through gaps and acrylic is high, and air temperature control is infeasible. (Right) GRObot shown with added Reflectix insulation, which makes temperature control manageable. Light leakage is lowered, as side windows are covered and reflectivity of walls is high.

2.2.2 Water Temperature Control

An air to liquid heat exchange system was implemented for reservoir water temperature control. For the second trial, the water temperature was maintained at 20°C. An Allied Thermal Designs 140W Dual In-Line Peltier Chiller/Heat Pump is used for water cooling. A Grove DS18B20 temperature probe is submerged in the nutrient water, which is well-mixed and of uniform temperature, and serves as feedback for the microcontroller. A proportional control system scales the duty cycle of the Peltier chiller from zero to full power according to the magnitude of the error in measured temperature to set temperature. Thermal energy from the Peltier is picked up by a closed loop of water circulating through 6' of ¼" outer diameter copper tubing which is submersed in the nutrient water. Flow through the closed loop is generated with an Active Aqua 250 GPH submersible pump. The Arduino code is given in the Appendix.

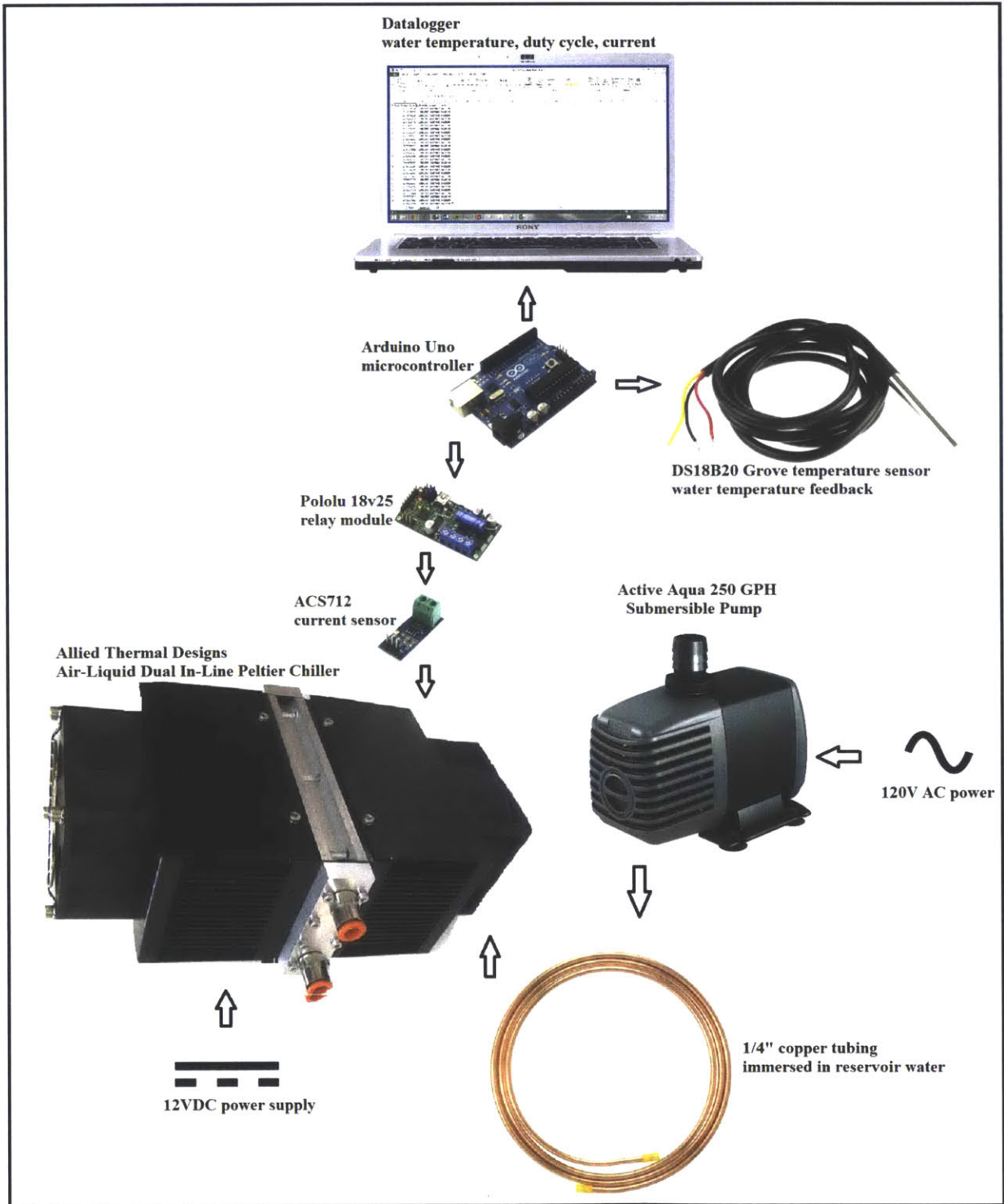


Figure 2-8: Schematic of water temperature control system. The microcontroller takes water temperature as input and scales the error from the set point temperature in order to command the Peltier to heat or cool and with what intensity. The gear pump circulates water through the Peltier to the copper tubing which is submersed in the nutrient water. Power requirements are logged by a watt meter in-line between the DC power supply and Peltier chiller.

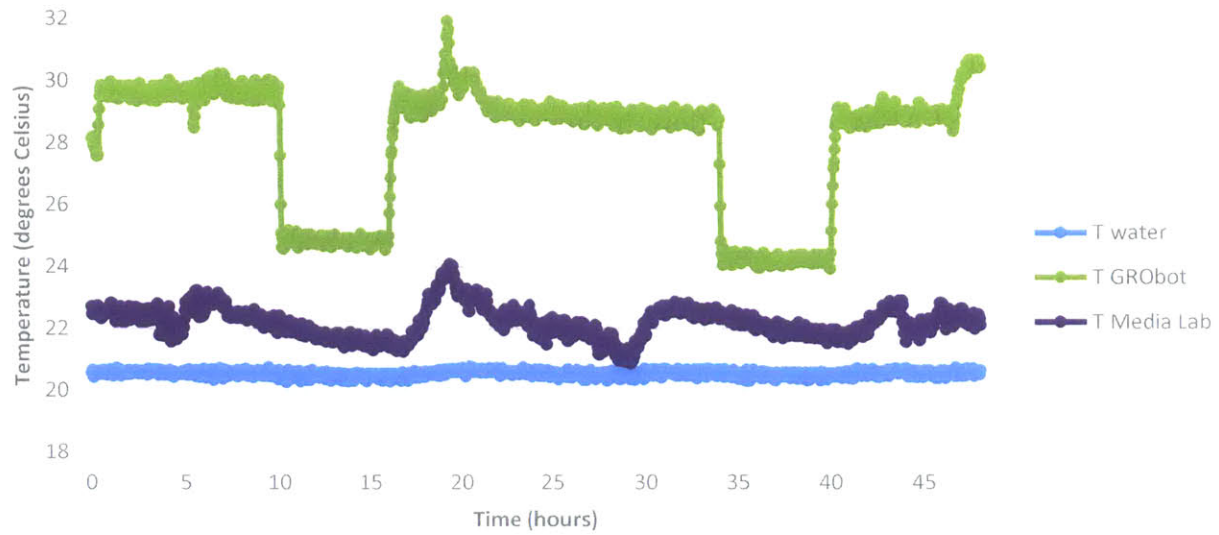
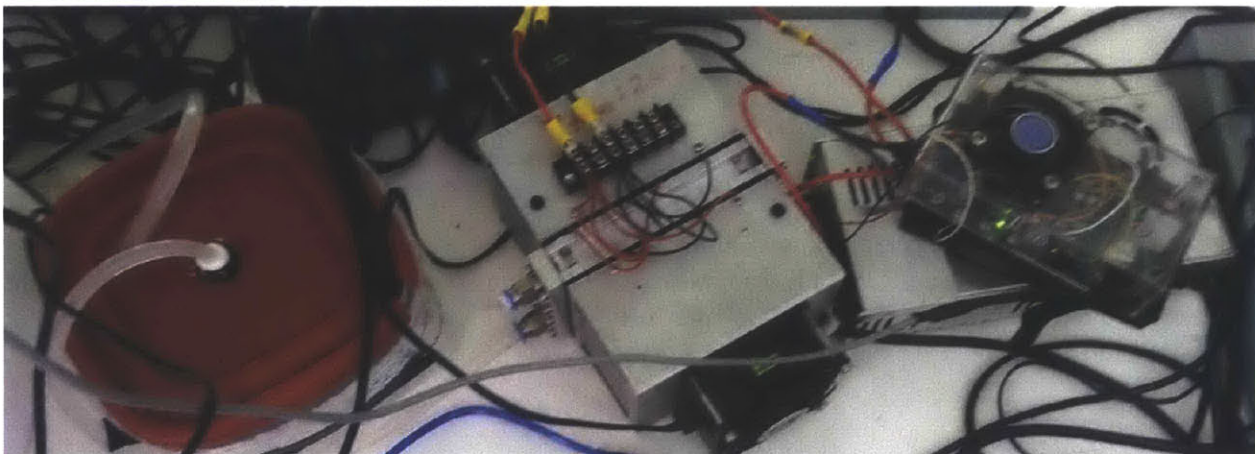


Figure 2-9: Temperature measurements of the Media Lab 5th floor CityFARM space, air inside GRObot at the Styrofoam tray, and water in the hydroponic reservoir. With the air and water temperature control systems installed, the air inside GRObot maintains 30°C during the day and 25°C at night, with the water kept at approximately 20°C.



Figure 2-10: (Left) Hydroponic reservoir with water temperature control system installed. The copper coil can be seen through the bubbles created by the air stones. (Below) Components of water temperature control system exterior to GRObot. On the left is the container which houses the submersible pump, with inlet and outlet lines seen emerging from the top. The Peltier chiller is shown in the center. The inlet line is connected to the pump, and the outlet line goes to the copper coil. On the right, the controller is shown sitting on top of the Peltier's power supply.



2.3 Root Zone Temperature Experiment Procedure

Caesar basil were planted from seed, one seed each in 54 Horticulture foam substrates, and placed into the CityFARM ebb and flow hydroponic system that is used as a germinator, propagating plants until mature enough for transplant into the façade farm. The basil were left in an ebb and flow system similar to the one drawn in Figure 1-1 (Bottom Left) for two weeks. In this system, the pH is maintained near 6 and the electrical conductivity is kept between 0.8 and 1.5 mS/cm. The pumps turn on for three minutes three times per day at 09:00, 15:00, and 21:00, filling the trays with nutrient water. The plants still have access to water and nutrients when the pumps are off, as the Horticulture retain water. The air temperature stays near 33°C, and the water temperature near 21°C. The fluorescent lights are on 18 hours per day from 06:00 to 24:00.



Figure 2-11: (Top Left) Ebb and flow seedling propagation system with fluorescent lighting. (Bottom Left) Layout of five basil samples ready for mass, stem length, and number of leaves measurement. (Right) Seedlings pulled out of ebb and flow system after two weeks of growth.

After two weeks in the ebb and flow system, the basil seedlings were removed, and the forty healthiest plants were chosen to continue. Five of the forty plants were taken for measurements of initial mass and length from beginning of root development to top of stem. These measurements were destructive, as the roots that had grown into the Horticultures were removed before measurement. Then, the rest of the 35 basil plants were transplanted into the GRObot, which was outfitted with the air temperature control system. Every other day, five basil plants were sampled at random for measurements. The reservoir water was kept between a pH of 6 and 6.5 and electrical conductivity between 1.2 and 1.5 mS/cm. Three Vernier temperature probes continuously logged the temperatures of the water, the air temperature at plant level, and the Media Lab space in which GRObot was placed. At the end of two weeks of growth inside the GRObot, the last five plant measurements were taken and the trial ended. These steps were repeated for comparison of basil growth in a trial with root zone water temperature maintained at a chilled 20°C.

3. Thermal Characterization of GRObot

In the two-week control trial, 35 two-week-old basil seedlings were transplanted into the air-temperature-controlled GRObot environment without temperature control of the water in the hydroponic reservoir. Data collected on fluctuations of GRObot air temperature, water temperature, and ambient Media Lab temperature were analyzed in order to create a model to predict the amount of energy necessary to maintain water temperature at a constant 20°C throughout another two-week basil growth trial in GRObot.

Dominant thermal resistances affecting temperatures of interest were determined in order to create an applet, which future GRObot users might use to predict energy consumption based on changes made to their GRObot system. Additionally, this applet can be optimized for use in other crop production scenarios and is tested on a hydroponic system in a greenhouse setting with weather data input.

3.1 Determining Thermal Resistance Dictating Water Temperature

A steady-state approximation for the power required to control water temperature was sought, according to the resistance circuit drawn in Figure 3-1. R_{total} includes the contributions of the following thermal resistances: conduction through the 1” Styrofoam plant tray, potential air convection on the top of the tray, convection of the water circulating on the underside of the Styrofoam, and radiation from the LED panel; all in parallel with the evaporation and transpiration resistances. It is assumed that no heat transfer occurs through the sides and bottoms of the water reservoir as these surfaces are insulated with Reflectix. $T_{styr.surface}$ corresponds to the air temperature inside the GRObot at the top surface of the Styrofoam tray, referred to more simply as T_{GRObot} .

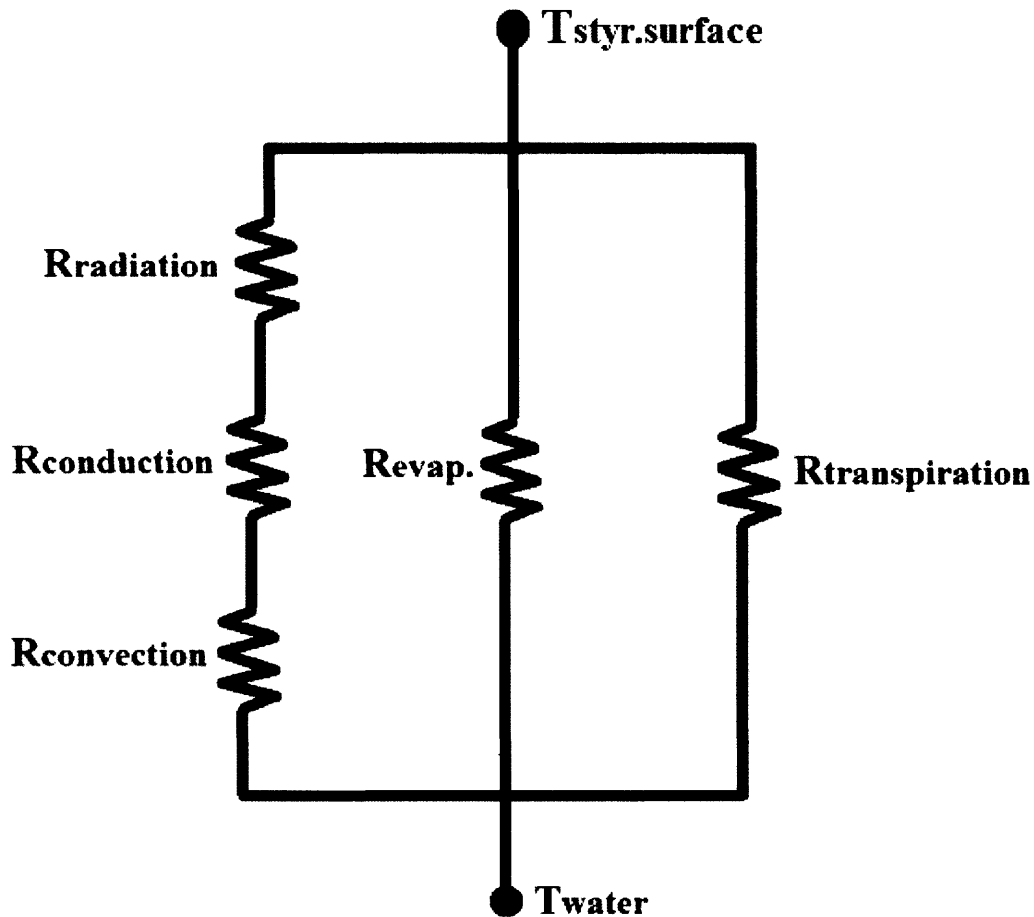


Figure 3-1: Thermal resistance network for R_{total} , which encompasses the radiation, conduction, and convection resistance components in series, in parallel with the thermal resistances associated with evaporation and transpiration.

A transient model was employed to determine the R_{total} resistance, which combines the contributions of conduction, convection, radiation, evaporation, and transpiration to heat transfer between the T_{water} and T_{GRObot} nodes. T_{GRObot} and T_{water} data were taken from the experiment without water temperature control. A daytime section was chosen, in which T_{GRObot} was held at an average of 28.9°C, and T_{water} gradually rose over the 11.5-hour period examined, without external water temperature control.

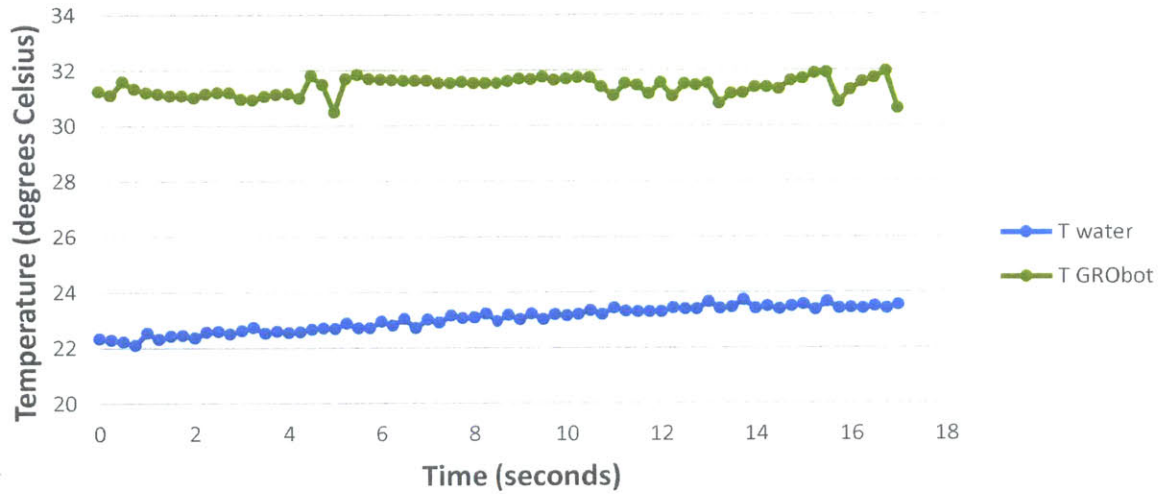


Figure 3-2: A segment of daytime temperature data from the experiment with air temperature control and without water temperature control used to determine the thermal resistance governing the reservoir water temperature.

With the aquarium pump circulating the reservoir water and the air pump continuously aerating, T_{water} is uniform throughout the reservoir and a function only of time. These conditions allow for use of a lumped system analysis in modeling R_{total} . The lumped parameter solution follows the form:

$$\frac{T(t) - T_{\infty}}{T_i - T_{\infty}} = e^{-\frac{t}{\tau}}$$

Equation 3.1

$$\tau = mc_p R_{total}$$

Equation 3.2

In this application, $T(t)$ corresponds to $T_{water}(t)$, T_{∞} to the average T_{GRObot} , and T_i to $T_{water}(t=0) = 22.31^{\circ}\text{C}$. The time constant, τ , is a function of the mass of water in the reservoir, $m = 17.2 \text{ kg}$, the specific heat of water, $c_p = 4187 \text{ J/kgK}$, and the thermal resistance, R_{total} . Taking the natural log of both sides of Equation 3.1 allows for a linear fit to a plot of the natural log of the non-dimensional temperature versus time, corresponding to the inverse of τ . The plot follows

$$\ln\left(\frac{T_{water}(t) - 28.9}{22.31 - 28.9}\right) = -\frac{1}{\tau}t$$

Equation 3.3

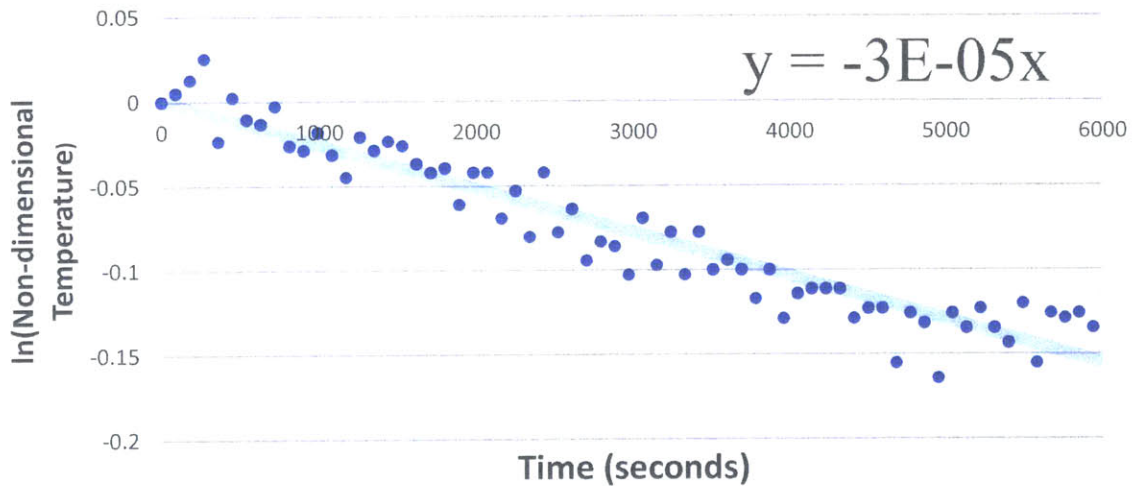


Figure 3-3: Based on the temperature data from Figure 3-2 and using Equation 3.3, the plot graphs the natural log of the non-dimensional temperature versus time and displays the fit used to determine the exponential time constant.

According to the linear fit,

$$\tau = \frac{1}{3 \times 10^{-5}} \text{ sec}$$

Equation 3.4

Using Equations 3.2 and 3.4, R_{total} becomes 0.46 K/W . The same process was used to analyze another section of daytime T_{GRObot} and T_{water} data. The same time constant and corresponding thermal resistance was found. Averages these values for thermal resistance and their respective errors yields a final R_{total} value of $0.46 \pm (1.3 \times 10^{-5}) \text{ K/W}$.

3.2 Calculating Energy Required for Reservoir Water Chilling

The steady state model was used to predict the amount of energy required for the Allied Thermal Designs Air-Liquid Dual-In-Line Peltier Chiller to maintain the reservoir water temperature at $T_{water, set} = 20^{\circ}\text{C}$. The model yields the following expression for power, $\dot{Q}_{thermal}$, required to maintain the water at T_{set} .

$$\dot{Q}_{thermal} = \frac{T_{GRObot} - T_{water, set}}{R_{total}}$$

Equation 3.5

Equation 3.5 is used to calculate the total predicted energy required for water temperature control over a two-week period, first based on a model of perfect air temperature control and second based on the air temperatures obtained in the two-week trial with air temperature control and without water temperature control.

3.2.1 Energy Required for a System with Ideal Air Temperature Control

Figure 3-4 shows the GRObot air and water temperatures over a 24-hour period with ideal air and water temperature control systems, with air temperature maintained at 30°C from 06:00 to 24:00 and 25°C from 24:00 to 06:00 and water temperature at a constant 20°C . Figure 3-5 then shows the power, \dot{Q} , required to combat the heat input from T_{GRObot} to T_{water} and chill the water to T_{set} . This \dot{Q} is calculated, neglecting transients, using Equation 3.10, which under these ideal control system conditions becomes

$$\dot{Q} = \frac{T_{GRObot} - 20}{0.46 \frac{\text{K}}{\text{W}}}$$

Equation 3.6

where $T_{GRObot} = 30^{\circ}\text{C}$ during the day and 25°C at night.

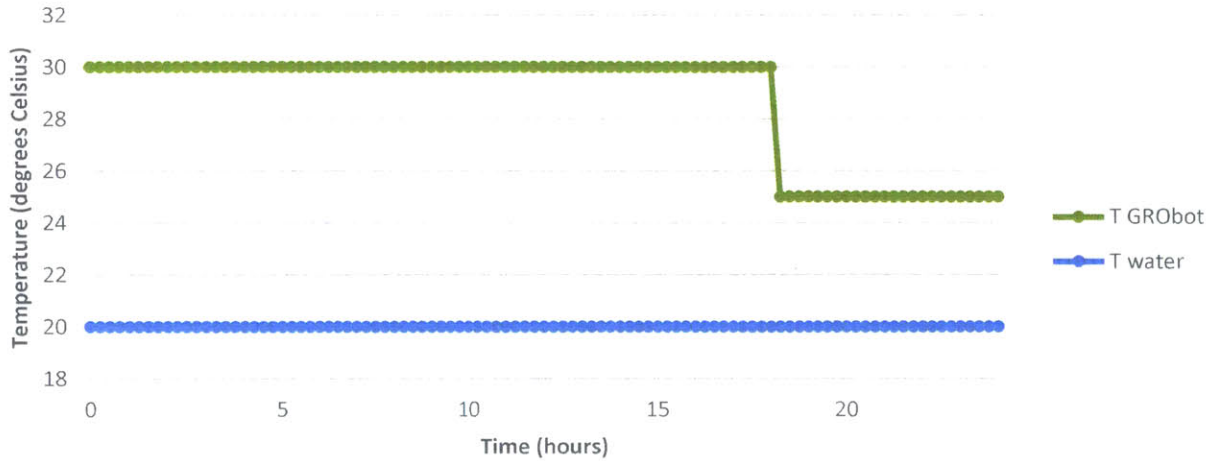


Figure 3-4: A 24-hour segment of simulated GRObot air and water temperatures based on perfect air temperature control, where the set temperatures of 30°C in the daytime and 25°C at nighttime are maintained.

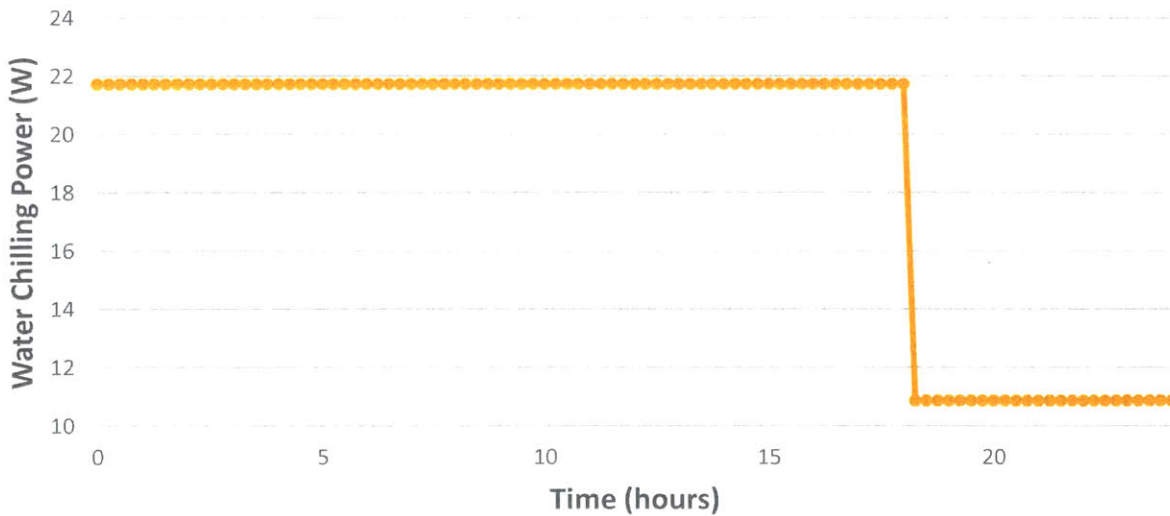


Figure 3-5: The water chilling power required of the Allied Thermal Designs Air-to-Liquid Dual-In-Line chiller to maintain water temperature at a constant 20°C calculated using Equation 3.6 and the simulated temperature data shown in Figure 3-4.

The area under the curve in Figure 3-5 represents the total thermal energy required for water chilling over a 24-hour period. The calculated total chilling energy for a 24-hour period with perfect air temperature control is 0.04 kWh. Stretched across a time period of two weeks, the amount of time each basil trial is conducted in GRObot, the energy required to chill the water adds

up to 0.63 kWh. Taking into account the chiller’s coefficient of performance, $COP = 0.55$, and using Equation 3.7

$$Q_{electrical} = \frac{Q_{thermal}}{COP}$$

Equation 3.7

the daily electrical power consumption is 0.08 kWh, and the electricity consumption over two weeks is 1.23 kWh. With an average Massachusetts electricity cost of 14.91 ¢/kWh, a day of water temperature control should cost 1.2 ¢, and two weeks of water temperature control should cost 18 ¢ more than the case without water temperature control.³⁷ The average instantaneous electrical power consumption is 34 W.

3.2.2 Energy Required for a System Based on Experimental Data

The air temperature control system does not function perfectly and therefore, the case for chilling the reservoir water for measured air temperatures is analyzed. Figure 3-6 shows a 24-hour section of the data, with imperfect air temperature control. Figure 3-7 then shows the power, $\dot{Q}_{thermal}$, required at each time to combat the heat input from T_{GRObot} to T_{water} and chill the water to T_{set} . This $\dot{Q}_{thermal}$ is again calculated using Equation 3.6.

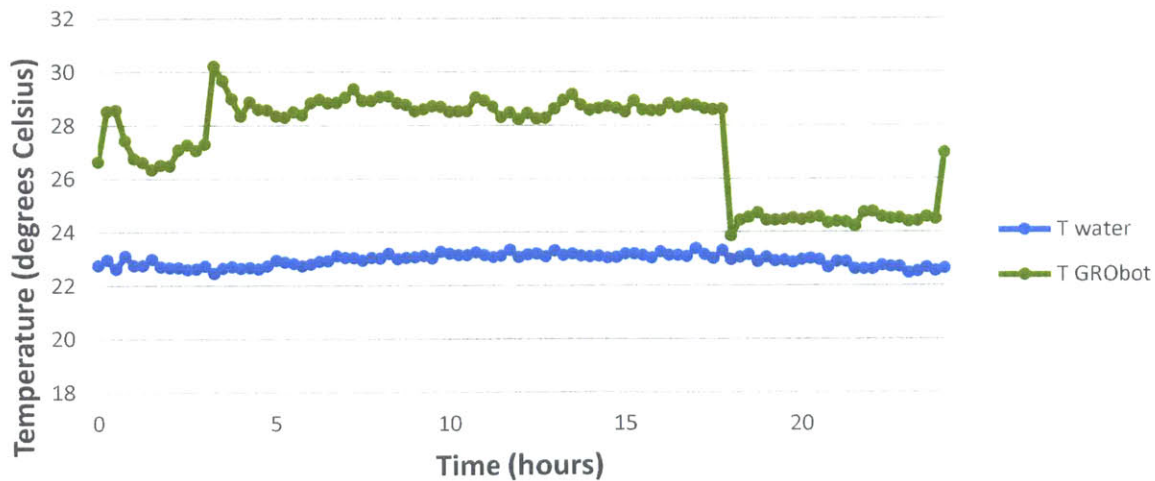


Figure 3-6: A 24-hour segment of GRObot air and water temperatures from the experiment with air temperature control and without water temperature control, where the set temperatures of 30°C in the daytime and 25°C at nighttime were not perfectly maintained.

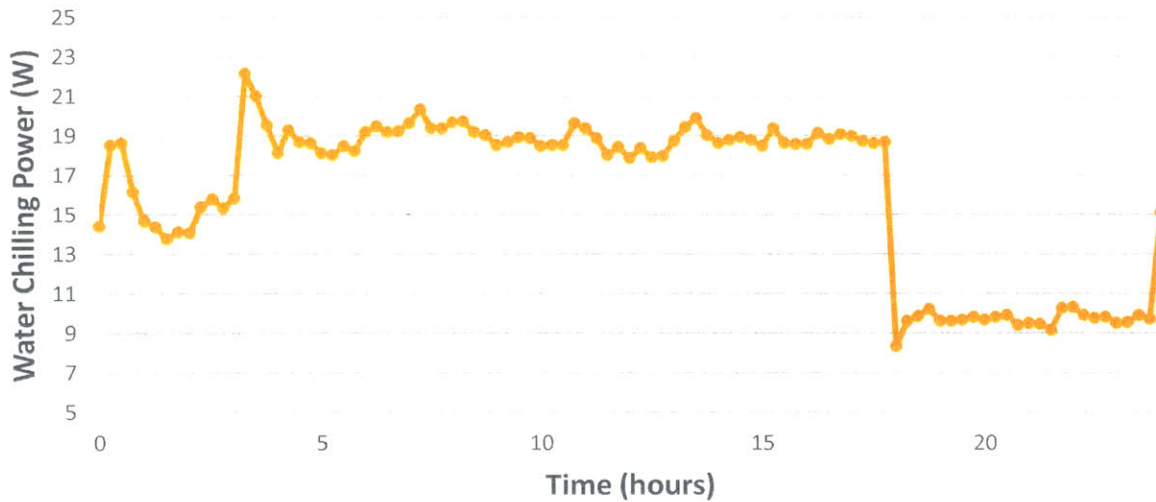


Figure 3-7: The water chilling power required of the Allied Thermal Designs Air-to-Liquid Dual-In-Line chiller to maintain water temperature at a constant 20°C calculated using Equation 3.6 and the actual experimental data shown in Figure 3-6.

For the example 24-hour data shown in Figure 3-7, it would have taken 0.03 kWh to maintain the reservoir water at $T_{set} = 20^{\circ}\text{C}$. Doing the same analysis on the full two weeks of imperfect air temperature control data, the total energy it would have required to maintain the reservoir water at $T_{set} = 20^{\circ}\text{C}$ is calculated to be 0.51 kWh. Using Equation 3.7, the electrical power necessary for 24 hours of water chilling and two weeks of water chilling are 0.05 kWh and 0.92 kWh, respectively. This corresponds to 0.81 ¢ and 13 ¢ worth of electricity, respectively. The average instantaneous electrical power consumption required for chilling throughout the two-week period is approximately 30 W. These calculations fall below the predicted requirements found in Section 3.2.1 using idealized air temperature data, due to the fact that the air temperature control system usually fell just below the day and night set point temperatures, making the temperature difference between the air and water smaller.

3.3 Interactive Applet: Calculating Energy Required for Environmental Control

An interactive applet for calculating GRObot energy consumption based on system control and material properties was created with Processing. With the first version of the applet presented here, users can change the duration of the daytime and nighttime settings; choose ambient, inner

GRObot air, and GRObot water temperatures; and specify the jacket material, thickness of the jacket, surface area of GRObot, and mass of water used. Each of these parameters is input into the steady state model derived in Section 3.2 in order to find energy required to maintain the specified water temperatures inside GRObot. The energy required to maintain air temperature is also estimated, based on calculations described further in this section. By allowing the user to change the surface area of the jacket and mass of water used, the applet can be applicable to the GROlab and GRObig scales. A change in the mass of the water could also be relevant to a new irrigation module, such as nutrient film technique (NFT) shown in Figure 1-1, which would require less water than a shallow water culture system. Certain crops' environmental recipes will call for specific temperature recipes. The applet can take such recipes as input and tell a user how much the crops will cost based on the expected growth time of the crop. Overall, the applet is meant as a tool for growers in predicting the effects of new modules or different environmental recipes on their energy requirements.

Because this applet accounts for energy required for air temperature control as well as water temperature control, the thermal resistance, R_{air} , between T_{GRObot} and $T_{Media Lab}$ had to be approximated. R_{air} consists of the resistances of the 1/4" thick acrylic and 5/16" thick Reflectix in series. The specifications of the Reflectix are not specific about R-value, as the value depends on the application. Because Reflectix radiant barrier insulation is composed of a layer of air trapped between two very thin reflective layers, the thermal conductivity of the Reflectix is assumed to be $k_{air} = 0.03$ W/mK. The thermal resistance, R_{air} , is approximated as the conductive resistance through the Reflectix, as acrylic is highly thermally conductive, with a thermal conductivity, $k_{acrylic}$, of 0.2 W/mK. Therefore, this upper resistance between $T_{Media Lab}$ and T_{GRObot} , R_{air} , is dominated by the following conductive resistance:

$$R_{air} = \frac{L_{Reflectix}}{k_{air}A_{surface}}$$

Equation 3.8

where $L_{Reflectix} = 5/16''$ is the thickness of the insulation, and $A_{surface} = 1.3$ m² is the surface area of GRObot over which heat transfer occurs. The resultant R_{air} is approximately 0.24 K/W.

The applet handles the inputs according to the resistance network shown in Figure 3-8.

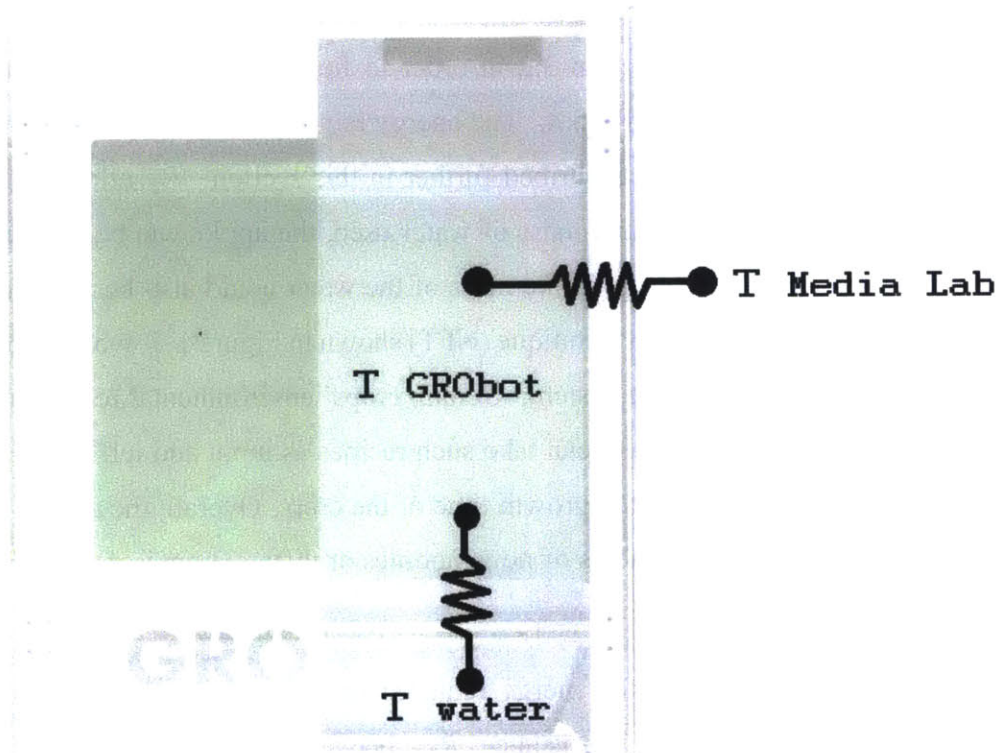


Figure 3-8: Thermal resistance network for the steady state model of heat transfer contributions to GRObot air and water environments. R_{air} includes conduction resistances through the acrylic and Reflectix layers in series, while R_{total} consists of contributions from plant transpiration, evaporation, and conduction through Styrofoam in parallel. R_{total} was calculated in the prior section.

Each thermal resistance, R_{air} and R_{water} , is calculated using the temperature, material, and water mass inputs according to Equations 3.2 and 3.8. Then, the thermal power for water temperature control is calculated using Equation 3.6, and the thermal power required for air temperature control is calculated using Equation 3.9,

$$\dot{Q}_{thermal} = \frac{T_{Media\ Lab} - T_{GRObot}}{R_{air} = 0.24 \frac{K}{W}}$$

Equation 3.9

These thermal powers are calculated for the user-specified daytime and nighttime conditions, and with user input for the duration of growth cycle, the applet outputs the energy required for environmental control. The Processing code is presented in the Appendix.

The applet outputs thermal energy required as opposed to electrical energy, as the *COP* varies with system component choices, which are not controllable through this version of the applet, though future implementations could include a library of commonly used pumps, lights, and heat exchangers and associated *COPs*. Therefore, the electricity cost output provided would have to be divided by the *COP* of the air and water temperature control systems in place. While the *COP* of the Peltier chiller used for water temperature control in the current GRObot system is known, that of the air temperature control system is not yet known. Further characterization of the air temperature control system consisting of the two computer fans and personal heater is ongoing.

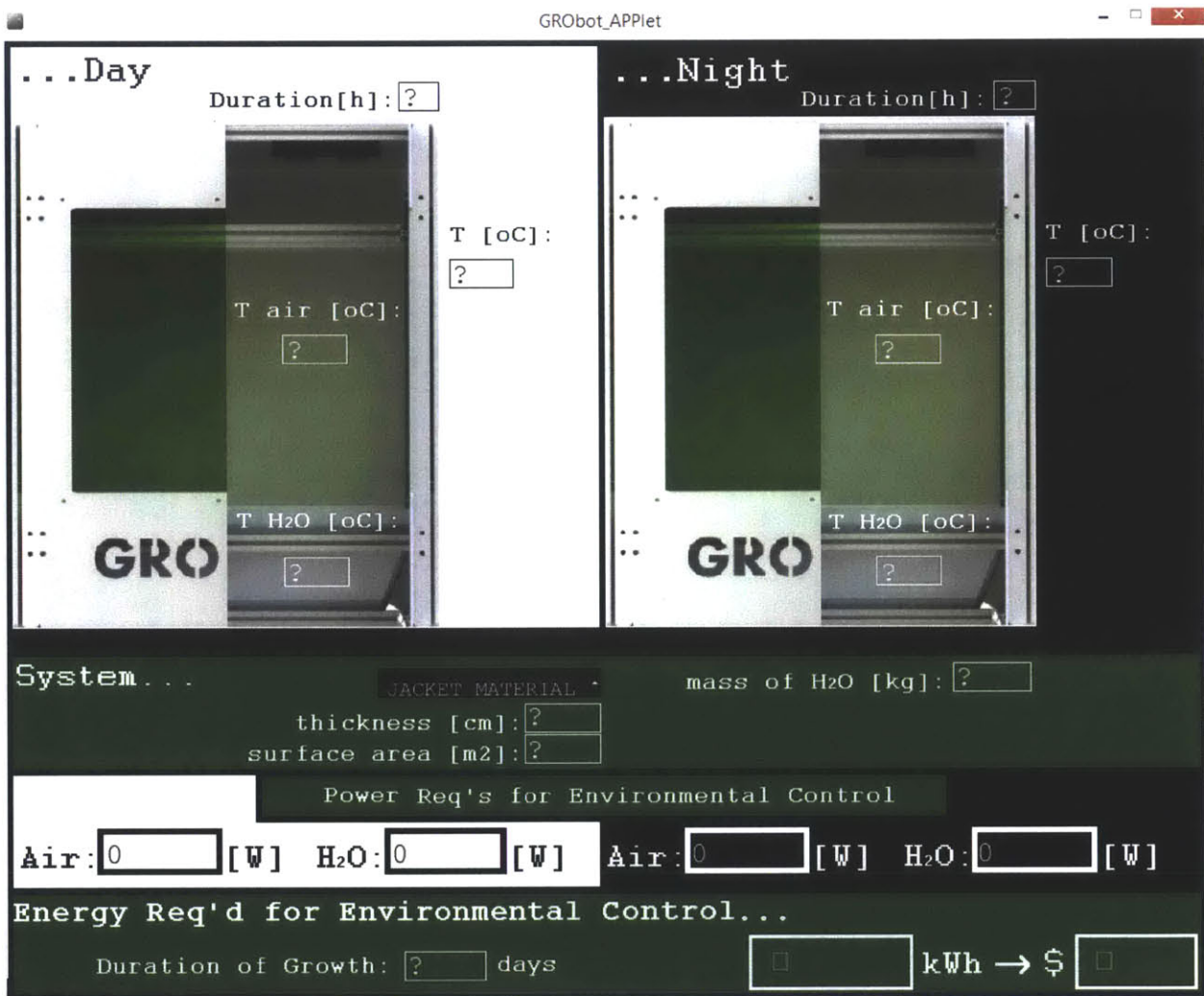


Figure 3-9: The default screen of the applet. All fields with “?” require user specification, and the drop-down menu headed “Jacket Material” allows for choice of acrylic, Reflectix, Styrofoam, or wood. Once all required values have been input, the fields with units [W], [kWh], and [\$] are automatically filled.

Inserting the conditions used for the RZT experiment conducted on GRObot for this study – a daytime GRObot air temperatures of 30, nighttime air temperature of 25, and constant water temperature of 20 – yields the following result. The ambient temperatures input are the average daytime and nighttime temperatures recorded in the lab space surrounding GRObot. Reflectix is chosen as the jacket material over acrylic due to its dominant thermal resistance in the in-series resistance of the jacket. As discussed in Section 2.2.1, the control system had insufficient power for air temperature maintenance of the GRObot with a jacket comprised only of acrylic. The calculations shown in Figure 3-10 Table 3-1 further demonstrate the value of the added Reflectix layer.

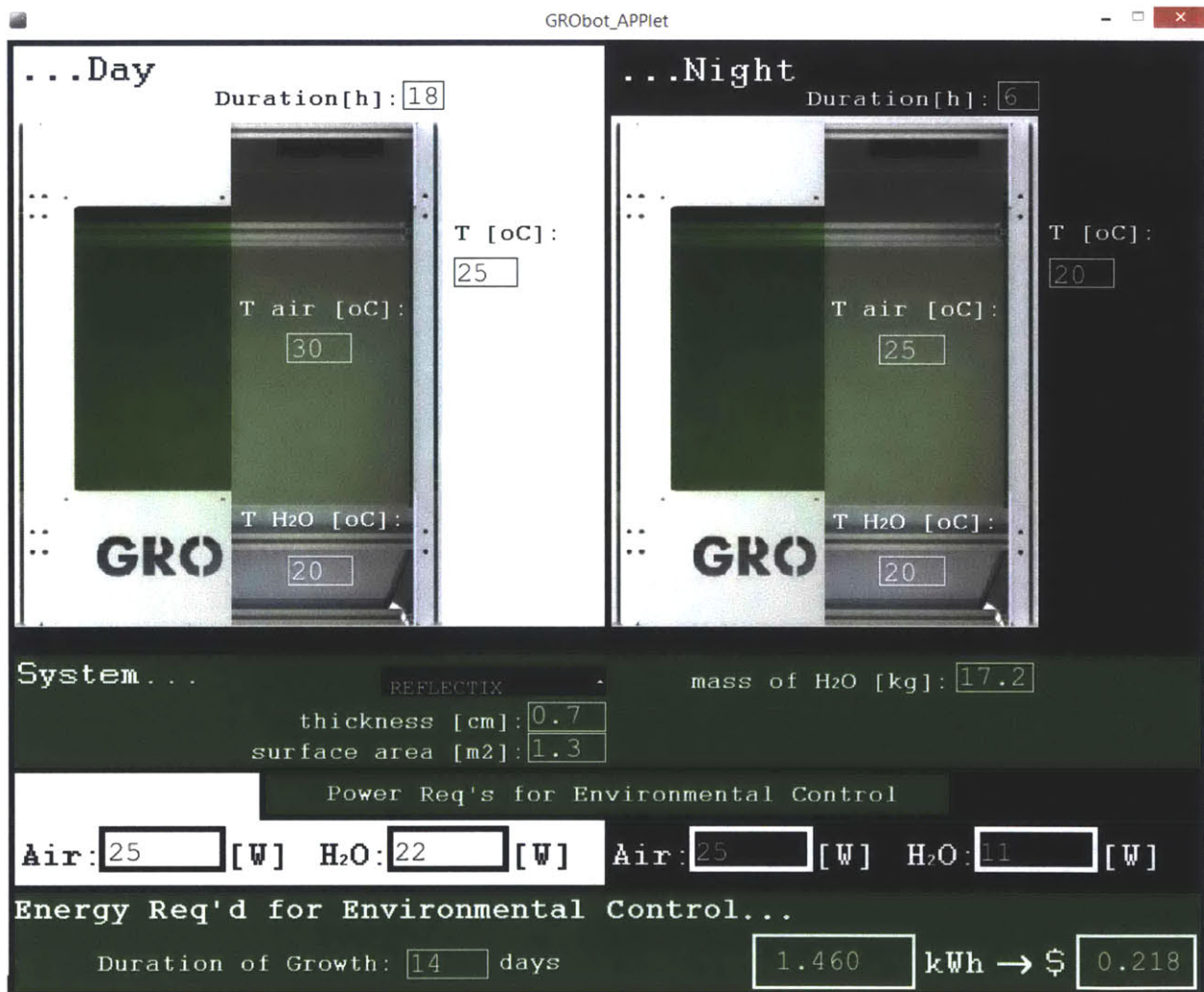


Figure 3-10: Inputs mimicking the root zone temperature chilling experiment conducted on GRObot in this study. The thermal power requirements for the GRObot air and water temperature controls during daytime and nighttime are displayed, followed by total thermal energy required for a two-week duration of growth. The energy required is converted to cost based on the average Massachusetts cost of electricity, however the efficiency of the thermal management systems is not included in the calculation.



Figure 3-11: A drop-down list displays material choices for the GRObot jacket outer. Each material is associated with its thermal conductivity, which is used to update R_{lower} .

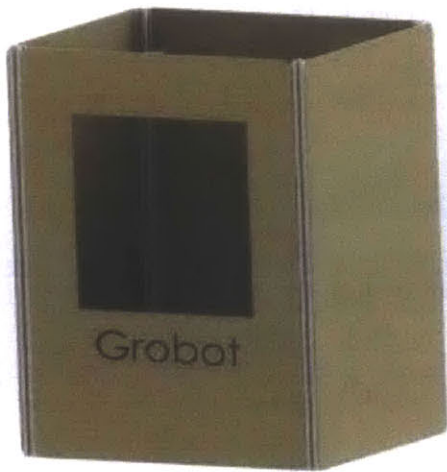


Figure 3-12: The applet’s option for changing the outer jacket material reflects the expectation that users will want to customize the aesthetic of their GRObots. Emma Feshbach, another CityFARM researcher, has already begun prototyping other jacket designs, such as this 1/8” thick birch jacket. A user deliberating the effects of switching the jacket material can use the applet to determine its effects on the energy cost of environmental

Table 3-1: Energy required for GRObot environmental control for two weeks based on different jacket material choices. All other parameters were kept constant, with temperatures, jacket thickness and surface area, water mass the same as shown in Figure 3-10.

Material	Thermal Conductivity [W/mK]	Energy Req’d for Environmental Control [kWh]
Acrylic	0.20	6.87
Reflectix	0.02	1.46
Styrofoam	0.03	1.66
Wood	0.05	2.19

As energy costs are still a major hurdle in CEA and vertical farming, it is the hope that this applet can evolve as the GRObot hardware and power requirements evolve, allowing users a

reliable prediction of energy costs. While this version factors power consumption only of the environmental control systems, a next more thorough energy audit applet will include the needs of the air pump, water circulation pumps, and lighting. The energy requirements for these components are shown in Table 3-2. This and future, more thorough versions of this applet can be a major resource for those seeking ways to cut down their GRObots' energy costs. Users have this tool for virtual experimentation with different irrigation systems, tweaking environmental recipes, or switching out components.

Table 3-2: Energy requirements of components not included in the applet energy calculations which only account for components involved in air and water temperature control. The electrical energy use for a 24-hour period is based on a daytime length setting of 18 hours.

Component	Electrical Power Consumption [W]	Status	Electrical Energy Use in 24 hrs [kWh]
Air pump	18	Always ON	0.04
Water circulation pump	5	Always ON	0.01
Peltier chiller water circulation pump	16	Always ON	0.03
LEDs	75	Daytime ON, Nighttime OFF	0.18

3.4 Case Study: RZT Control for a Hydroponic System in a Greenhouse

A RZT experiment was installed at the Ecological Greenhouse of Kibbutz Ein Shemer in Israel, inside of which two identical shallow water culture hydroponic systems were set up to grow lettuce, one with water temperature control maintaining 25°C and one without water temperature control. The water aeration and circulation scheme is the same as shown in Figure 2-3, and the water temperature control, which required only heating, was accomplished with a resistive heating component normally used for fish tank heating. Two 1” thick Styrofoam containers comprise the reservoirs, which hold 33 L of water each. Air temperature is a function of greenhouse

temperature, as the hydroponic systems are not directly enclosed as seen in the setup shown in Figure 3-13.

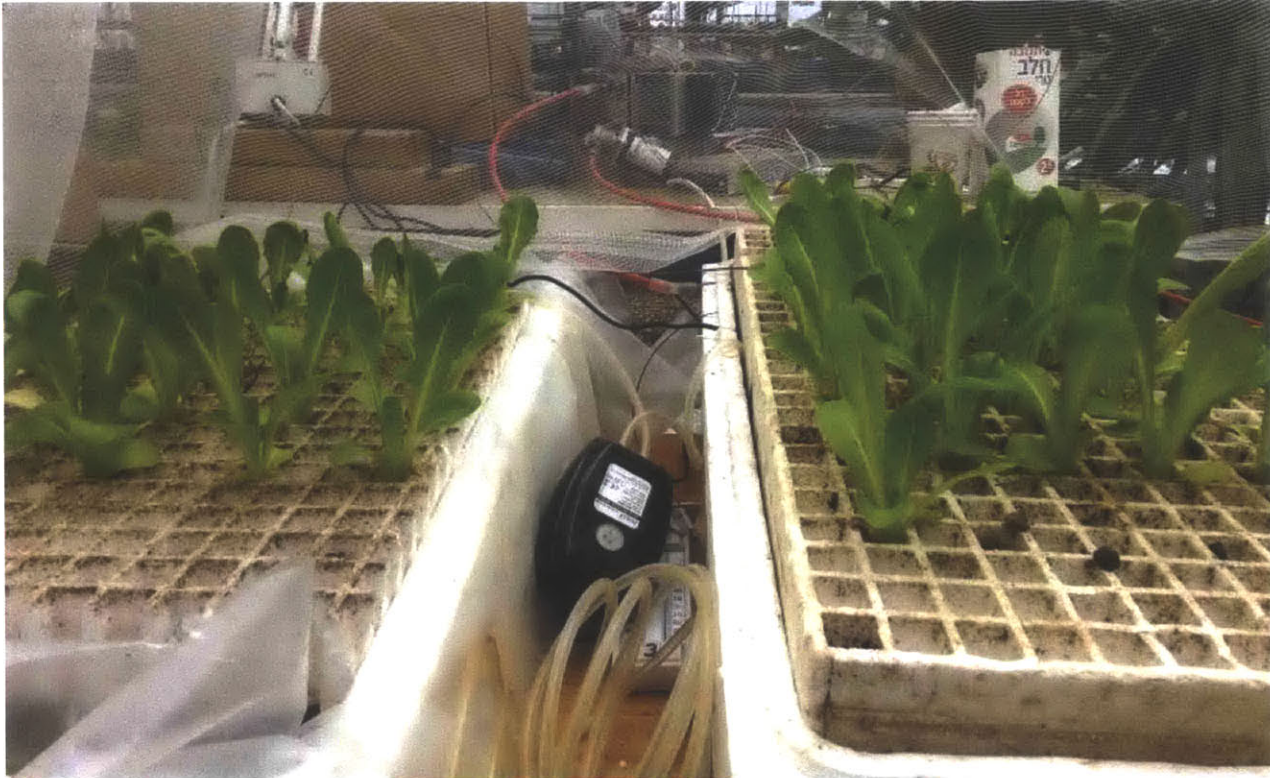


Figure 3-13: The shallow water culture hydroponic systems set up in a greenhouse to examine the effects of RZT warming on lettuce growth. The water temperature in the setup on the left is allowed to fluctuate with air temperature, while the setup on the right is rigged to maintain a constant water temperature of 25°C using the Allied Thermal Designs Dual-In-Line Peltier Chiller shown on the back table with red tubing leading to a submersed copper coil. The air pump is placed between the Styrofoam reservoirs, with lines leading to each reservoir.

A steady state model approach similar to that derived in Sections 3.1 and 3.2 is applied to this setup, as a case study for scaling work done first explored on the GRObot to the GROlab, GRObig, and greenhouse scales. Figures 3-14 and 3-15 show example daytime air and water temperatures and solar irradiation data for a 10-hour period in the greenhouse. The air temperature and solar irradiance measurements are obtained at the height of the hydroponic systems.

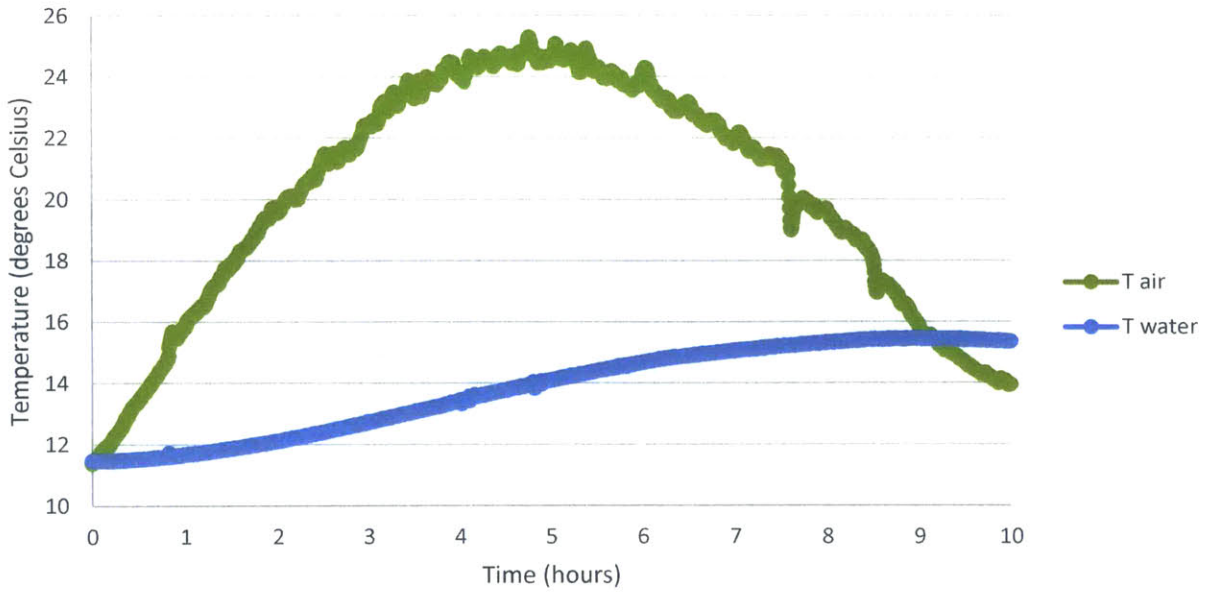


Figure 3-14: Daytime air temperatures inside the greenhouse at the level of the lettuce in the hydroponic systems and water temperature inside well-mixed reservoir over a 10-hour period.

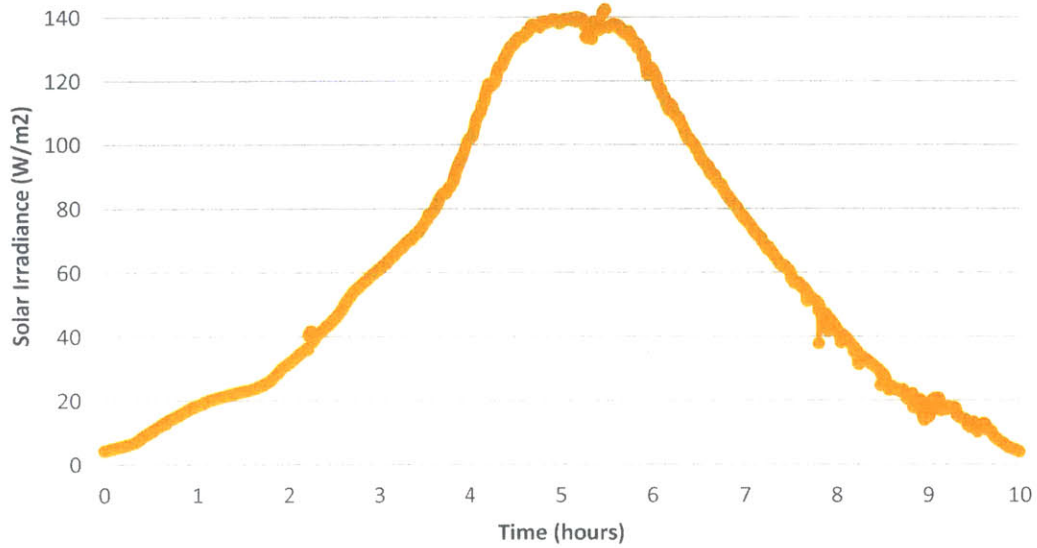


Figure 3-15: Daytime solar irradiation inside the greenhouse measured at the level of the lettuce in the hydroponic systems over a 10-hour period.

As a very basic estimate for the thermal resistance between the air and water temperature nodes, the average heater power required for water temperature control and the average difference between the air and water temperatures for a daytime period are input to Equation 3-10,

$$\dot{Q}_{heater} = \frac{T_{air} - T_{water}}{R}$$

Equation 3.10

where the average daytime air temperature from Figure 3-14 is $T_{air} = 20.0\text{ }^{\circ}\text{C}$, the average daytime water temperature is $T_{water} = 13.8\text{ }^{\circ}\text{C}$, and the average heater power necessary for daytime heating is determined based on the data shown in Figure 3-16, which begins data collection at 09:00. From the daytime data, which is comprised of the initial dip in heater power, the average power required is approximately $\dot{Q}_{heater} = 15\text{ W}$. The resulting thermal resistance, calculated using Equation 3-10, is then approximately 0.4 K/W.

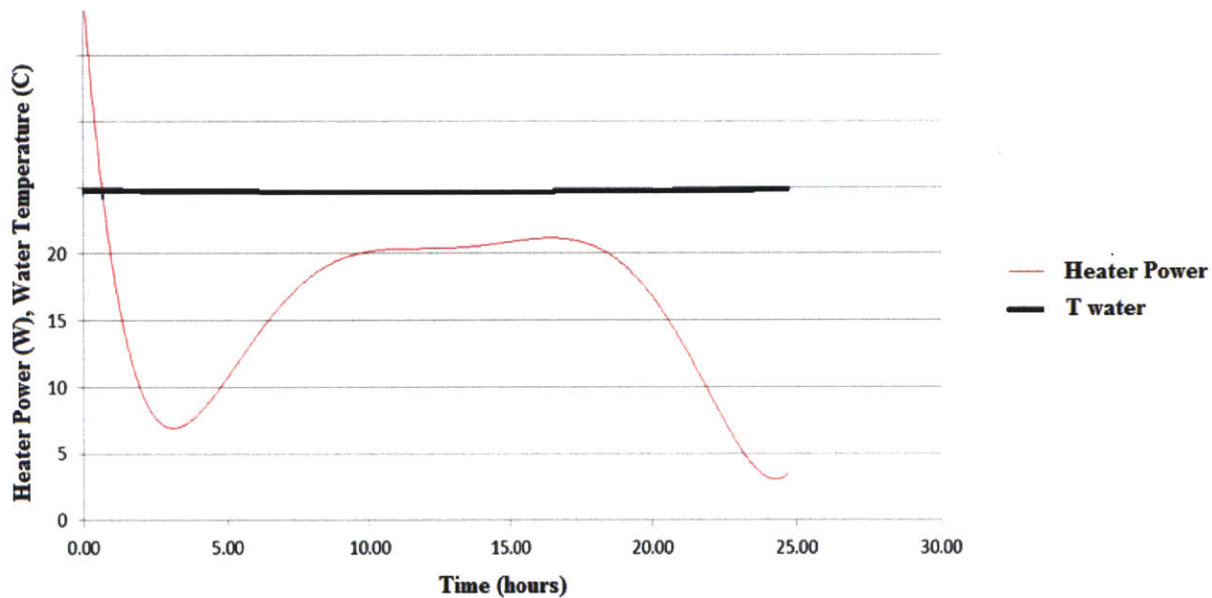


Figure 3-16: Fish tank heater power shown in red is monitored over a 24-hour period in the greenhouse. The water temperature controlled to 20.5°C is shown in black.

This thermal resistance can then be input to the applet as the resistance dictating the power required for water temperature control based on the user’s specified desired air and water temperatures. In the future, to go a step further in functionality of the applet, solar irradiation data

can be input to the model. For example, using the solar irradiation measurements shown in Figure 3-15, the air temperature at the height of the hydroponic systems shown in Figure 3-14 can be derived. Because the solar irradiation measurements shown in Figure 3-15 are taken at the height of the hydroponic systems, in order to use solar irradiation tables from weather models as input, the stratification of air temperature at different heights in the greenhouse must be measured, as shown in Figure 3-17, to determine the thermal resistance between the greenhouse roof and the top of the Styrofoam plant trays of the hydroponic systems.

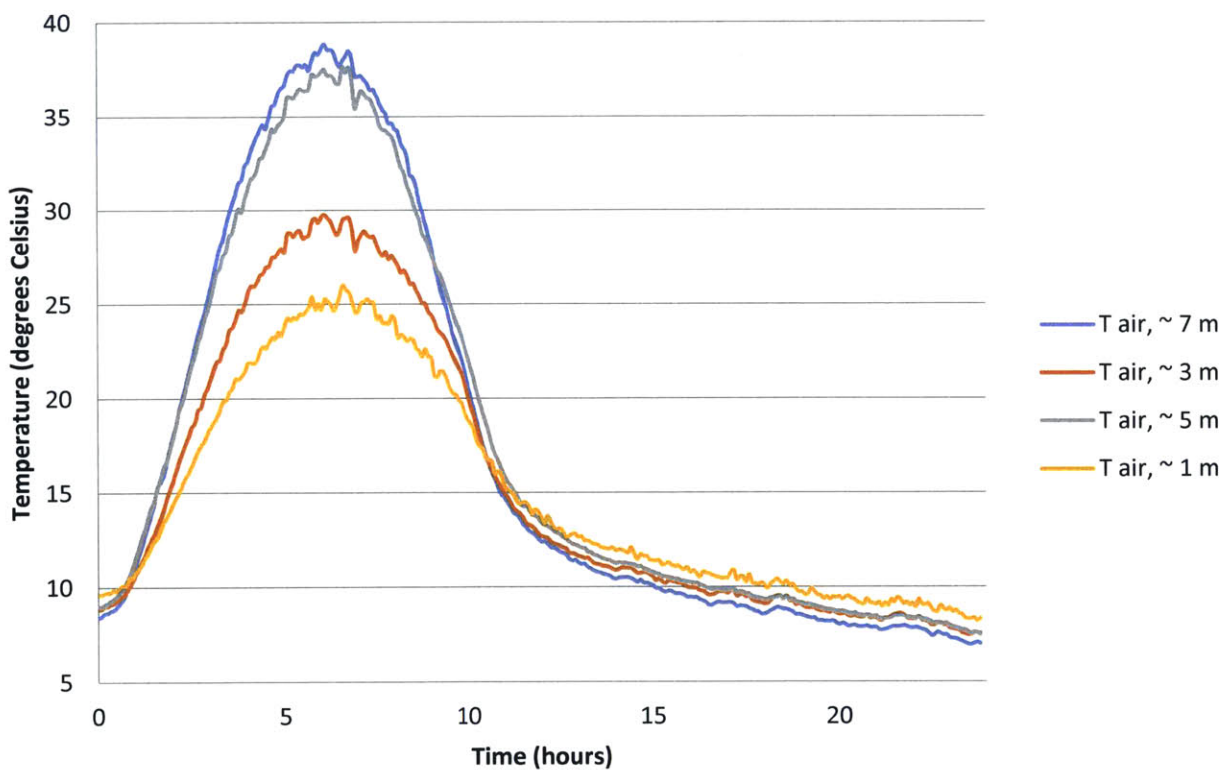


Figure 3-17: Air temperatures inside the greenhouse at different levels. The air is not well-mixed and therefore would have to be treated as separate stratification levels in order to find a total thermal resistance of the air between the greenhouse roof and the level of the hydroponic systems.

The diagram in Figure 3-18 illustrates the heat transfer components acting on the control volume of the hydroponic reservoir water.

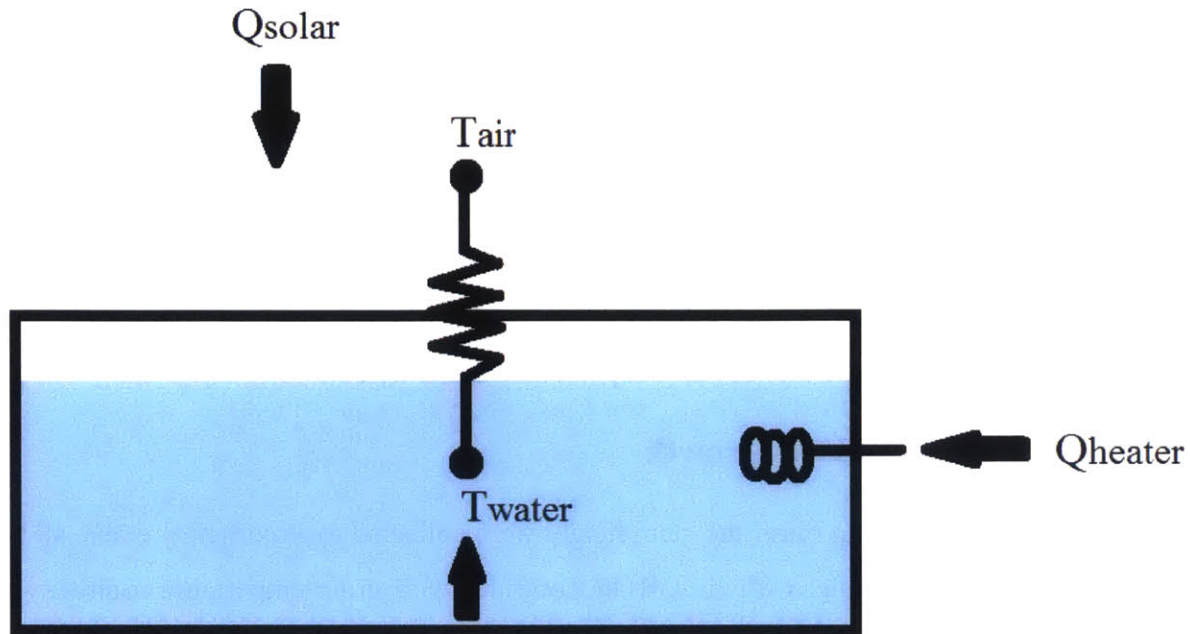


Figure 3-18: Heat transfer modes acting on the control volume of a hydroponic reservoir water placed in the greenhouse. Heat transfer across the air-Styrofoam-water boundary which is characterized by conduction through the Styrofoam and convection on both sides of the Styrofoam as well as radiation heat transfer which is transmitted through the Styrofoam.

From this diagram, the equation describing heat transfer on the control volume is

$$Q_{solar} - Q_{water,loss} + Q_{heater} = 0$$

Equation 3.11

where Q_{solar} incident on the Styrofoam surface would be calculated using air temperature stratification information such as the data in Figure 3-17, and the heat transfer due to the radiation transmitted through the Styrofoam to the water would be calculated based on the emissivity of the Styrofoam tray. $Q_{water,loss}$ would be approximated based on the thermal resistance calculation shown in Equation 3.10 or done more accurately based on the transient case demonstrated in Equations 3.1 and 3.2. Then, Q_{heater} could be solved for in order to determine energy requirement for water temperature control. This variation of the steady state model demonstrates the potential for using solar irradiation tables as input for predicting the thermal management requirements for a GROlab, GRObig, or greenhouse placed outside anywhere in the world.

4. Experimental Results

Data on basil growth in the GRObot at two different RZT conditions were examined. In the first trial, water temperature was allowed to fluctuate while in the second, water temperature was controlled to approximately 20°C. Data on both basil growth and energy consumption of the water temperature control system were recorded. Effects of water chilling on basil growth are discussed as well as comparison of the measured energy consumption of the water chiller to the consumption predicted via the thermal model presented in Section 3.

4.1 Effects of RZT on Basil Growth

Data on basil seedling mass and stem height were collected approximately every 48 hours during two two-week trials of growth in a GRObot outfitted with an air temperature control system. In the first trial, in which water temperatures were allowed to fluctuate according to the air temperatures inside the GRObot, an average temperature of 22.7°C with a standard deviation of 0.66°C was recorded. In the second trial, water temperature was maintained at an average temperature of 20.5°C with a standard deviation of 0.27°C was recorded. The mass and stem measurements documenting basil growth for the two trials are shown in Figures 4-1 and 4-2, respectively.

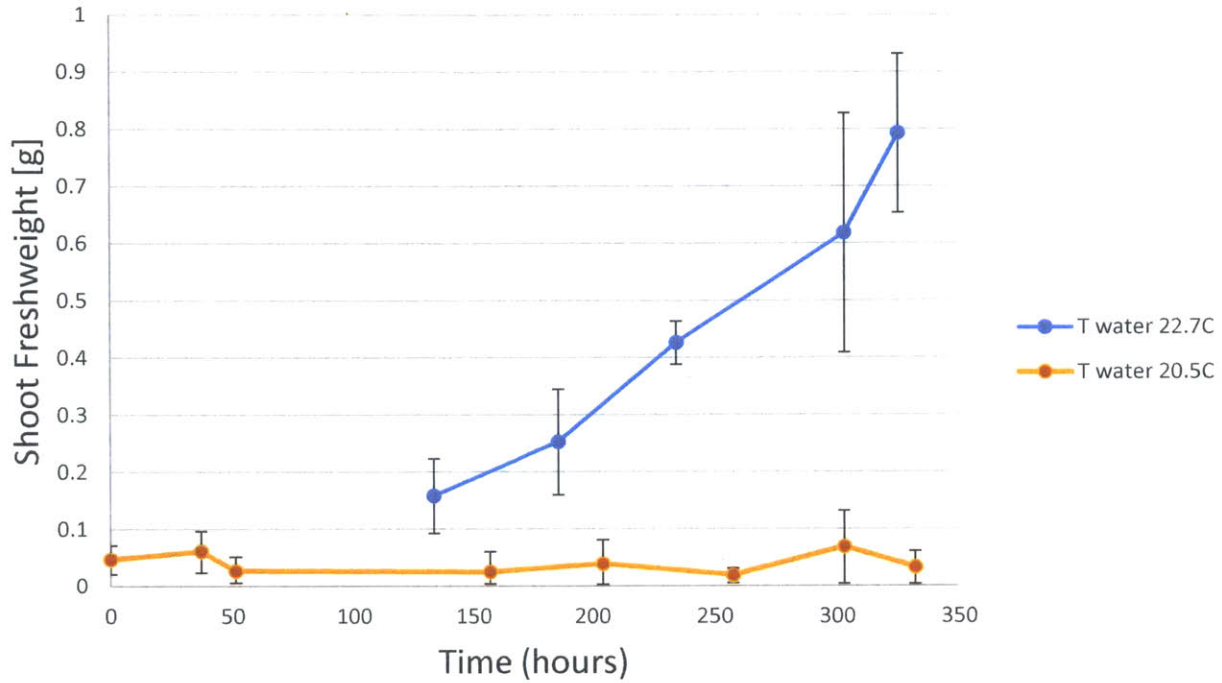


Figure 4-1: The freshweight measurements of basil seedlings at various stages of growth inside the GRObot. Each point averages the measurements taken on five samples at the respective timestamp. The data in blue corresponds to the experiment without water temperature control, and the data in orange corresponds to the experiment in which the RZT was chilled to 20.5°C.

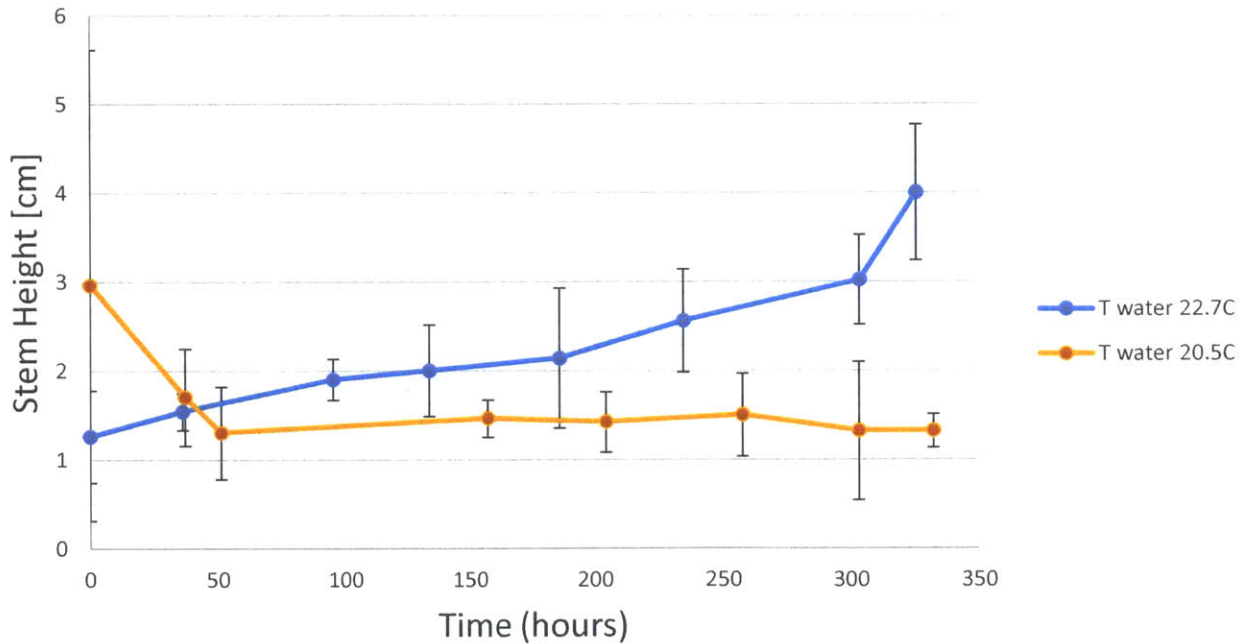


Figure 4-2: The stem height measurements of basil seedlings at various stages of growth inside the GRObot. Each point averages the measurements taken on five samples at the respective timestamp. The data in blue corresponds to the experiment without water temperature control, and the data in orange corresponds to the experiment in which the RZT was chilled to 20.5°C.

There is a clear difference in seedling growth rate between the two different RZT conditions, indicating that 20.5°C is below the minimum viable RZT for Caesar basil growth. As can be seen in Figure 4-1, the mass of the basil seedlings grown at the average RZT of 22.7°C exhibited the exponential growth expected of healthy plants. On the other hand, the mass of the basil seedlings grown at the RZT of 20.5°C did not increase over the two-week period, and the stem length even decreased upon transplantation into the GRObot with chilled RZT. This immediate decrease could be due to an initial transplantation stress from which the basil were not able to recover. In this case, 20.5°C may still be a viable RZT for basil if as suitable acclimation procedure is carried out. Another study conducted on effects of RZT on hydroponic growth, though tested on the *Betula pendula* Roth tree, is very telling of the sensitivity of plants to transplant conditions. In the study, seedlings stored cold experienced stunted growth at 6°C and no growth at 2°C. However, seedlings acclimated to a hydroponics system with an RZT of 17°C were able to withstand transplant into systems at 2, 6, and 12°C systems.³⁸ The study demonstrates the importance of properly preparing seedlings for future transplant conditions. Perhaps had the ebb and flow system temperature been lowered 1°C for the week prior to transplant into GRObot, the basil would have fared better. This would indicate the need to tune environmental recipes based on maturity and prediction of future stresses the plant will encounter.

Knowing that RZT and DO in the root zone are linked, a likely scapegoat for the poor growth of the basil with the chilled RZT is a mishap with aeration of the water. However, as seen in Figure 4-3, the basil in the chilled RZT case were exposed to higher levels of DO than the basil that grew exponentially due to the lower temperature and corresponding higher DO saturation level. The basil grown in the chilled RZT condition had access to more than sufficient DO for root respiration. For the RZT case in which the water temperature was allowed to fluctuate and in which the basil grew healthily, the average DO level was lower than that of the chilled RZT case. Therefore, it can be confirmed that the effect on basil growth is the RZT and not the DO level.

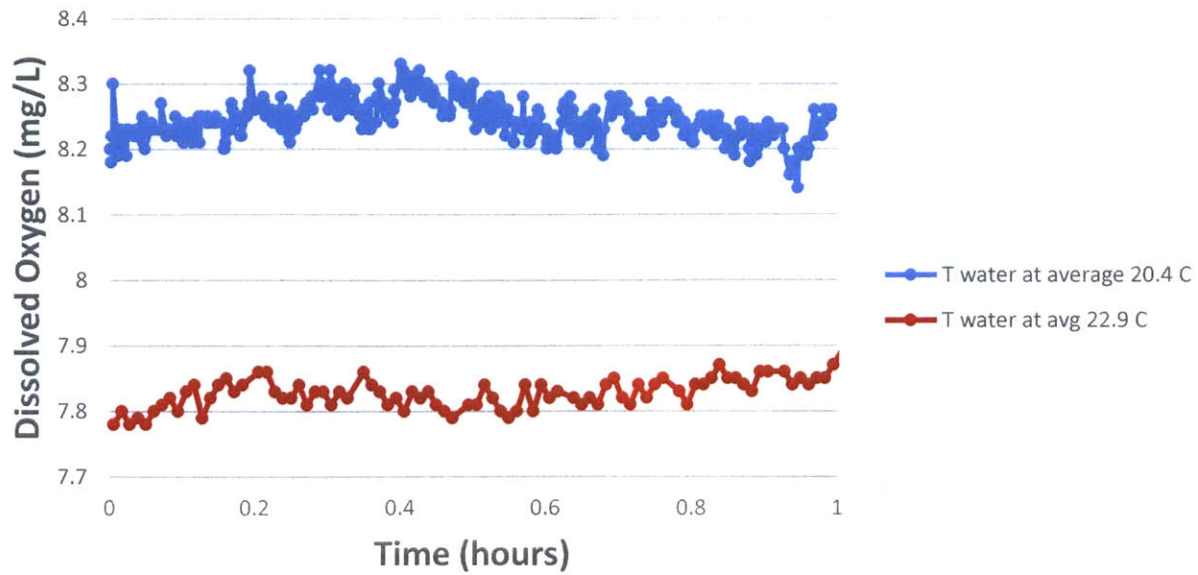
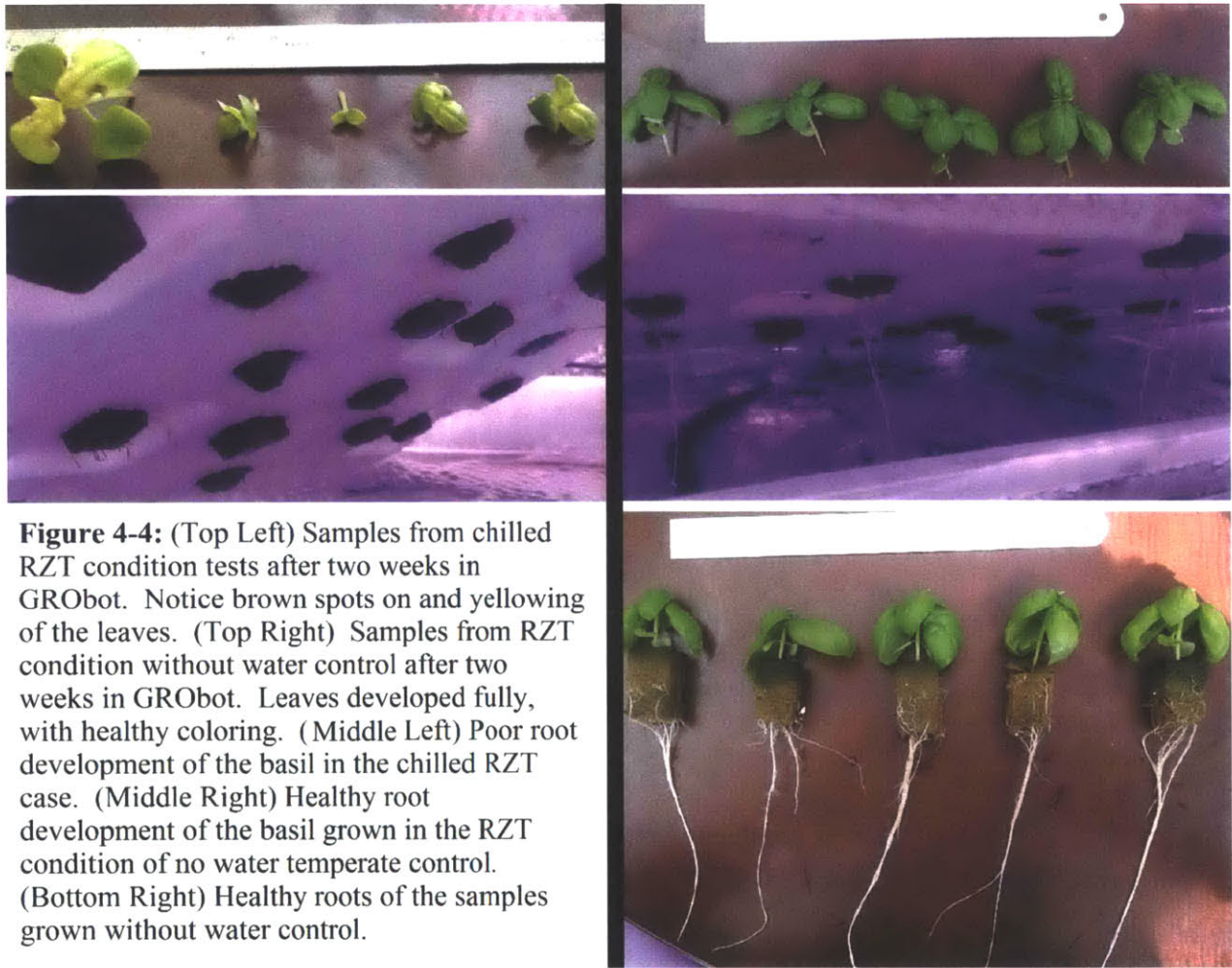


Figure 4-3: An hour of DO data for each RZT condition. The same aeration setup is used in both conditions – the air pump connected to submersed air stones, which bubble the reservoir water. As is expected due to the higher saturation potential of DO in colder water temperatures, the chilled RZT provided higher for higher concentrations of DO, shown in blue.

However, the basil grown in the chilled RZT conditions never created root systems which might have taken advantage of the high DO concentrations. This lack of a healthy root system inhibited water uptake rates, mirrored by the low growth rate and frequent drying up of the leaves, as well as nutrient uptake indicated by widespread yellowing of leaves. These conditions are shown in Figure 4-4. The basil samples shown have both been in GRObot for two weeks, but the basil subjected to a chilled RZT, shown on the left, developed fewer leaves and less mass than the basil with no water temperature control and higher average RZT.



The inhibited root growth seen of the basil grown in the chilled RZT condition could itself stem from poor water uptake. The dynamic viscosity of water increases as temperature decreases as shown in Figure 4-5, meaning that the plant would require more capillary force for water uptake the lower the RZT.

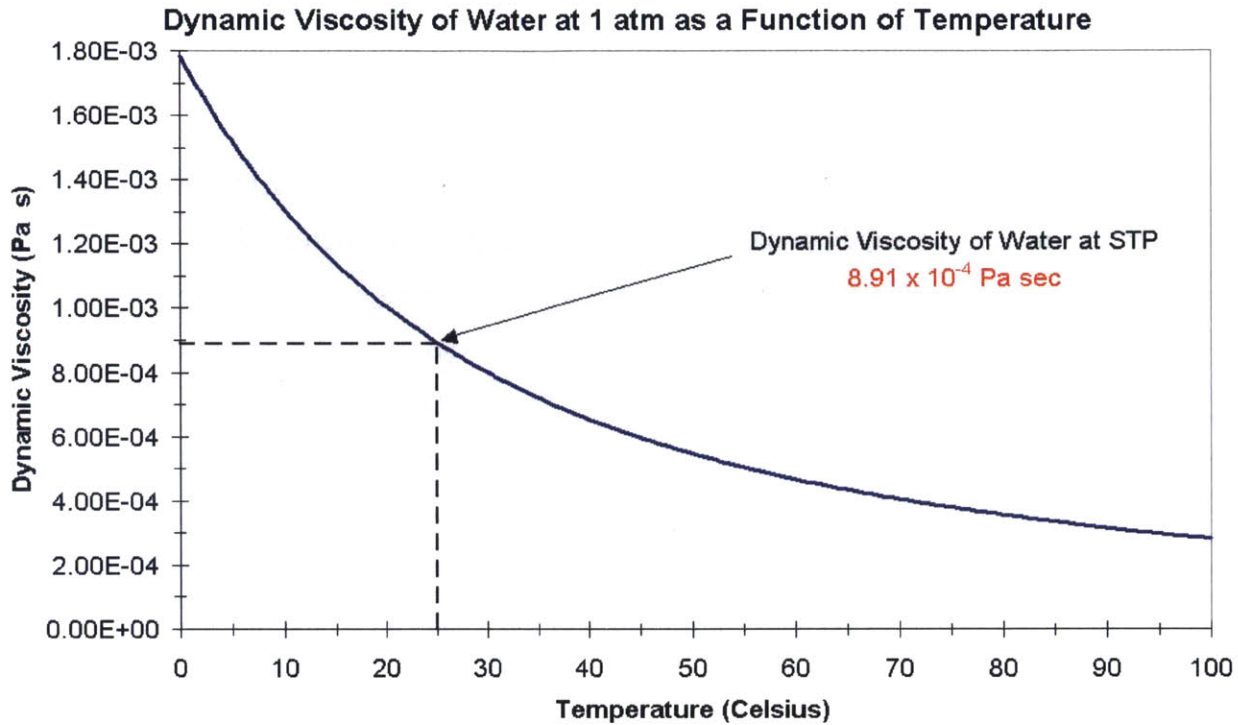


Figure 4-5: Dynamic viscosity of water decreases as a function of increasing temperature.³⁹ This fact may attribute to the poor root water uptake suspected for the basil grown in the chilled RZT condition.

With higher water viscosity, the cell membranes of the plant involved in water conduction may not function as efficiently.³⁸ However, these membranes that assist in capillary action may still be able to acclimate to compensate for slightly higher viscosities of water at lower temperatures, as indicated by the *Betula pendula* Roth discussed previously. Provided a suitable acclimation recipe which factors in plant maturity, current temperature conditions, future temperature conditions, and time to acclimate, 20.5°C may still be a RZT option for basil growth.

The ebb and flow system in which the basil seedlings were grown for two weeks from seed is kept near 21°C. If transplantation stress did indeed occur in the experiments conducted, then it may be an indicator that transplantation into a system with a similar or slightly warmer RZT is preferable to direct transplantation into a chilled RZT, even if the difference in temperature between the new and old farming systems is as small as 1°C. Because the seedling stage is the “most troublesome with regards to stressing or damaging” the plant, the propagation time in the

ebb and flow system might be extended to allow transplant of a more mature, robust plant.⁴⁰ Then, a gradual decrease in temperature might acclimate the plant for root water uptake at the set RZT.

These data presented on basil growth under different RZT conditions indicate either the impossibility of growth at RZTs 20.5°C and below or the need for proper acclimation procedures when chilling the RZT of a hydroponic system. The development of such acclimation recipes may allow plants to grow in unique conditions which allow for unusual multi-cropping arrangements. These tests conducted with air temperatures mimicking warmer climates, at 30°C during the daytime and 25°C at night, indicates that water cooling to a RZT as low as 20.5°C for a warmer climate crop such as basil can be destructive. Further temperature recipe experimentation at increments of higher RZTs is necessary to determine the range of viable RZTs for basil growth in warm air conditions. Additionally, further experimentation must be done to determine whether fluctuations in RZT are in fact beneficial to growth or the results presented here are simply due to the higher overall RZT in the condition without water temperature control.

4.2 Energy Consumption for Water Temperature Control

A GT Power RC 130A Power Analyzer Battery Consumption Performance Monitor was placed in series with the 12V 29A DC power supply and Allied Thermal Designs Dual-In-Line Peltier chiller in order to monitor electrical energy consumption of the water temperature control system. The energy consumption of the chiller attempting to maintain a RZT of 20°C was monitored over the course of five days. The electrical energy consumed over the period is graphed in Figure 4-6.

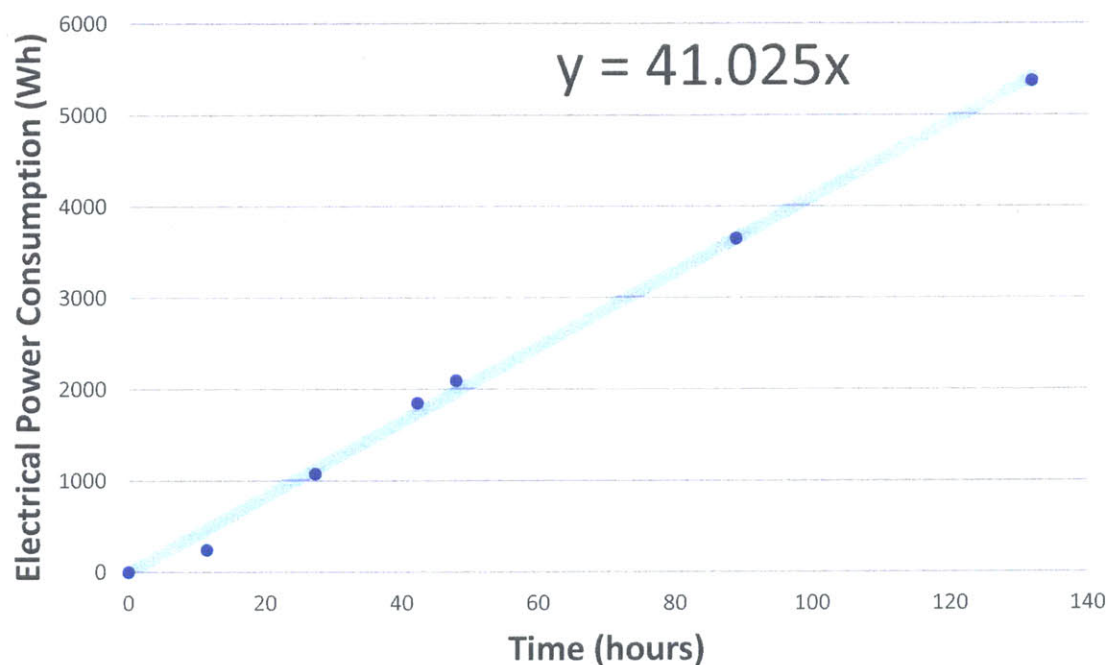


Figure 4-6: Electrical energy consumption of the water chiller over a five-day period. The slope corresponds to an average power usage of approximately 41W.

According to the calculations done through the applet, shown in Figure 3-10, the average expected thermal power requirement for water temperature control was 22 W during the daytime and 11 W at nighttime. For the Allied Thermal Designs Peltier Chiller with $COP = 0.55$, this corresponds to an expected electrical power requirement of 40 W during the day and 20 W at night. Therefore, on average, over the 24-hour period of which 18 hours is considered daytime, the predicted electrical power requirement for water temperature control is 35 W. The percent error

between the model-predicted average electrical power requirement and the measured average power requirement for water temperature control is 15%. For this case of water temperature control over a two-week period, which at an average of 41 W would have required a total of 1.3 kWh worth 20 ¢, the 15% error accounts for an unexpected extra electricity cost of 3 ¢. On this scale, such an error is acceptable. However, for GROlabs and especially GRObiggs in which commercial operations might be running, a 15% increase in expected overhead costs could be detrimental to business.

Examining the energy requirements for the components not involved in environmental control shown in Table 3-2, this percent error for the water temperature control energy requirement is rendered less significant. As can be seen in the right-most column of Table 3-2, the LEDs require the most energy per day over all other components, with 0.18 kWh per day. Altogether, environmental control system and other components included, one day of GRObot operation entails approximately 0.41 kWh. The 41 W required of the water temperature control system, which translates to 0.09 kWh per day, comprises only 21% of the total daily energy consumption. Therefore, the percent error due to the model's assumptions made in predicting water temperature control energy requirements is 3% in terms of overall expected cost.

For improved accuracy of the model, assumptions used to calculate the thermal resistance between the GRObot air and water temperatures in Section 3.1 should be explored. For example, a major environmental parameter affecting the thermal resistance to evaporation – relative humidity (RH) of the air – was not adequately measured, as the GRObot sensing systems did not yet have RH monitoring capability. Collecting data on the small fluctuations in RH due to air exchange with the external Media Lab will be used to improve the thermal model in the future. Furthermore, a true transient model should be developed such that the wave-like behavior of the water temperature due to turning on and off of the LEDs for daytime to nighttime switches and vice versa is emulated and used to predict a more sensitive power requirement for water chilling. The interactive applet will be improved according to a transient model and, upgraded to input location for the relevant electricity cost per kW, and evolve to accurately report energy consumption as the GRObot control systems evolve and span more parameters.

5. Future Work with GRObot

5.1 Hardware Developments

The CityFARM team plans to make GRObot hardware and software schematics available to users as an open source tool for CEA by the end of summer 2015. To prepare for this launch, the next iterations of the prototype will address necessary improvements to the temperature control systems, addition of new control systems, cost, and needs of users in different markets whether in schools, research labs, or in homes. The air temperature control system as it currently stands involves air exchange with the outside environment. In this case, an air conditioning system for particle removal and humidity control will be necessary. For certain users' needs, an air-tight system might be necessary for controlled experiments, in which case the jacket will need upgrading with pressure-fit walls, and a new temperature regulation system separate from the exterior will have to be installed. The current water temperature control system uses a heat exchanger overqualified for the power required for GRObot's requirements. A next iteration of the water temperature controls will require a 50 W chiller rather than the 140 W chiller currently used, which will save on the cost of the GRObot kit. Furthermore, additional air quality controls systems for humidity and air temperature control will be included as well as fertilizer dosing and pH balancing for the irrigation system. These systems will make up the basic model of the GRObot, with designs for new control systems uploaded for the open source community to use and improve upon as they come.

Cost concerns will be more heavily considered in next iterations, as the target for the basic GRObot bill of materials is \$500. The acrylic jacket will have to be replaced with a more reasonably priced material that is waterproof, has a low thermal conductivity, and is aesthetically pleasing. One iteration on the jacket has been done with 1/8" birch wood treated with a waterproof stain. The thermal performance of this and future jackets will have to be compared, though all modules will be made available for users to customize their jackets as they please, according to aesthetics and level of performance they require. Additionally, the structural material for the skeleton of the GRObot is currently 80/20 aluminum extrusion. To lower the cost associated with this skeleton, next iterations will look to cheaper structural options that still offer modularity. Another large cost lies in sensing. A basic sensing system should include sensors for air and water

temperature, carbon dioxide and humidity, and electrical conductivity and pH of the water. Several sensing suites have been designed for these purposes, though none have cost less than the target price for GRObot of \$500. Lowering this cost will require further research for available products on the market or in-house development of low-cost sensing systems.

5.2 Networking Capability

Future GRObots, GROlabs, and GRObiggs will include networking capabilities. Currently, the CityFARM façade farm reports its sensor data to the project's web application shown in Figure 1-4. This application is currently being upgraded to enable more interaction including the ability to track plant history such as transplant date and sensor data and click and drag of different plants into virtual trays to update the farm's crop inventory during a planting cycle. A yet unused tab in the application is for remote environmental control of the system, which taps into the larger development of importing and exporting digital environmental recipes. Because a large part of the vision for users is the ability to share sensor histories and resulting crop physiologies and tastes, an important step in the networking capability is the method of importing and exporting digital environmental recipes. On the ideal network, a GRObot user in Boston can search for a recipe for sweet butter crunch lettuce, find one from a GRObot user in San Francisco, download the recipe, and replicate it in her own GRObot. This will involve sending GRObot control systems the control parameters required to replicate the recipe. The form these parameters take is still being explored and will require development on the sensing, data manipulation, and data transfer aspects of networking capability research.

5.3 The Community Approach to CEA

It is the hope that through the open source release of the GRObot schematics, a community of builders, growers, students, researchers, and the curious will form around an online forum meant to facilitate sharing of digital environmental recipes, inventions of new features and modules, and growing advice. Through such a community of enthusiasts, research around CEA, soilless farming, and vertical farming could become more open and transparent and popularize these methods which are currently mysterious and daunting to many. Through forums which address different aspects of research such as cost reduction or public policy, these problems which are largely only addressed in academia and industry can be brought to the public eye for awareness,

brainstorming, and networking. Because it is going to take many types of people to bring advanced agricultural methods to the forefront of food production, a point source for ideation, collaboration, and research can spur a movement towards expanding sustainable farming faster. Whether with GRObot users supplementing their diets on a small scale or new operators creating businesses upon the GROlab or GRObig scales, these systems aim to be the first standardized platforms that together make a significant impact on reducing reliance on current unsustainable food production systems.

6. Conclusion

6.1 Building the First GRObot

A first GRObot prototype was built with a home, school, or research lab user in mind. The dimensions were chosen to fit on a standard countertop but allow for significant space for growing and adding on features. The outer jacket was built of acrylic for aesthetic purposes, with the Reflectix radiant barrier insulation being required for thermal management purposes. The jacket is meant to provide a cool aesthetic while also being approachable and amenable to the addition of new GRObot features. Windows on three sides were initially desired, however it was decided that the Reflectix should cover all but the front window for the sake of light retaining and thermal management. The first environmental control systems added were for air and water temperature regulation. The air temperature was either cooled via air exchange with the surrounding Media Lab air or warmed using a personal heater which blows warm air from a back corner of the GRObot. The fans and heater were switched on and off depending on feedback from a temperature probe on the top of the Styrofoam plant tray. Water temperature control was achieved with a closed loop of water circulating through a Peltier chiller and copper coil submersed in the hydroponic reservoir water. The chiller power was dictated by commands from a proportional controller. Additional features included in the first GRObot prototype were an LCD screen which reported air temperature and status of the air temperature control components as well as a webcam which sent pictures of the plants to a website every morning.

6.2 RZT Effects on Basil Growth

The effects of two RZT conditions were tested on basil growth in warm climate conditions. The first condition allowed the RZT to fluctuate according to the air temperature which was 30°C during the daytime and 25°C at night. This resulted in an average water temperature of 22.7°C over the two-week trial period. For the second RZT condition, which was compared with the first at the same air temperature conditions, the water temperature was set to maintain a constant 20°C RZT. The resulting average RZT over the two-week period was 20.5°C. The effects on basil growth were stark. The basil in the first condition in which RZT was allowed to fluctuate exhibited healthy exponential growth, while the basil whose RZT were chilled to 20.5°C fared poorly, showing no growth over the two-week period and exhibiting dysfunction in root water and nutrient uptake. The basil grown with the warmer RZT ended the two-week trial with fresh weight mass of 0.8 g and stem length of 4.0 cm compared to the 0.03 g and 0.18 cm of the basil grown with the chilled RZT.

This study demonstrates the importance of experimenting with environmental recipes for crops at different maturities as well as predictive recipes which might acclimate crops for anticipated future conditions pertaining to transplantation. Basil has been known to grow viably at RZT of 20°C. However, what environmental history might have allowed for this growth where growth did not occur with the same RZT recipe used in these GRObot experiments? Though the RZT experiments presented in this study may show that Caesar basil cannot grow in an RZT of 20.5°C, it may well be that with proper acclimation, a RZT of 20.5°C is within the viable range for basil growth.

This study suggests that acquiring environmental recipes for basil requires analyses with different plant maturities and histories of a crop's life. A range of parameters will not be as simple as an RZT between 21 and 30°C, air temperature between 25 and 30°C, DO between 5 and 8 mg/L, and so on. Such ranges will be more complex, requiring experimentation on the crop of interest at various maturities, acclimation requirements, *and* environmental parameters. With so many parameters and combinations to test for determination of viable ranges of environmental parameters, it would take a network of GRObots, GROlabs, and GRObigs to tackle a fully inclusive environmental recipe determination experiment for a single crop.

6.3 Thermal Characterization of GRObot

Using temperature data collected throughout the two two-week trials of RZT conditions on basil grown in the GRObot, a steady state thermal model was created in order to predict energy consumption of the environmental controls systems. The energy consumption of the air temperature control system was found to require more energy than the water temperature control system due to the low thermal performance of the jacket used for this prototype. The results of the model for the air temperature control system's energy consumption is not verified in this study, which focused more on the energy required of controlling the RZT. The model for the water temperature control system's energy consumption was compared to measurements of a watt-meter placed in series with the Peltier chiller and its power supply. It was found that the model predicted the energy consumption of the water temperature control system to within 15% of the measured value. For future developments of the model, the transient case should be considered to lower this error. A model that can predict the more gradual water temperature response to perturbations such as the LEDs turning on and off for example, can lower this percent error to obtain even more accurate energy consumption predictions.

The steady state model derived in this research was input to an interactive applet which users in the open source community might use as a tool for predicting their energy costs for certain environmental recipes. It outputs kWh and cents required to run the air and water temperature controls for specified day and night set temperatures for a specified duration of growth. As the extent of the control systems increases, this model will be updated to reflect the additional energy requirements. Also important to include will be the LED panel energy requirements, which are so far the bulk of the energy cost of GRObot operation. When a user wishes to import an environmental recipe into a GRObot, this applet can be an intermediate step in which the energy required to maintain the specified environment is automatically displayed to the user before final importation of the recipe. Additionally, if the recipe being imported has an associated expected yield of crop fresh weight, the applet can be used to calculate the cost per fresh weight of crop the GRObot is expected to produce. This open source applet is meant as a tool the community can use to easily predict important metrics of their CEA systems without having to delve into the thermal model itself.

Bibliography

1. World population projected to reach 9.6 billion by 2050 | UN DESA | United Nations Department of Economic and Social Affairs. (2013, June 13). Retrieved May 19, 2015, from <https://www.un.org/en/development/desa/news/population/un-report-world-population-projected-to-reach-9-6-billion-by-2050.html>
2. World's population increasingly urban with more than half living in urban areas | UN DESA | United Nations Department of Economic and Social Affairs. (2014, July 10). Retrieved May 19, 2015, from <http://www.un.org/en/development/desa/news/population/world-urbanization-prospects-2014.html>
3. Cloud, K. (2013, December 2). How Transportation Costs Affect Fresh Fruit And Vegetable Prices. Retrieved May 19, 2015, from <http://www.theshelbyreport.com/2013/12/02/how-transportation-costs-affect-fresh-fruit-and-vegetable-prices/>
4. Agriculture and Food Supply Impacts & Adaptation. (n.d.). Retrieved May 19, 2015, from <http://www.epa.gov/climatechange/impacts-adaptation/agriculture.html>
5. The Challenges of Producing Food on a Warming Planet. (n.d.). Retrieved May 19, 2015, from <http://www.climate.org/publications/ClimateAlerts/Summer2008/Challenges.htm>
6. Despommier, D. (2010). The vertical farm: Controlled environment agriculture carried out in tall buildings would create greater food safety and security for large urban populations. *Journal Für Verbraucherschutz Und Lebensmittelsicherheit*, 6(2), 233-236. Retrieved May 19, 2015, from <http://link.springer.com/article/10.1007/s00003-010-0654-3>
7. Gray, K. (2014, October 6). MIT's incubator-grown plants might hold key to food crisis (Wired UK). Retrieved May 19, 2015, from <http://www.wired.co.uk/magazine/archive/2014/10/features/server-farm>
8. Farming: Wasteful water use. (n.d.). Retrieved May 19, 2015, from http://wwf.panda.org/what_we_do/footprint/agriculture/impacts/water_use/
9. (n.d.). Retrieved May 19, 2015, from <http://howtogrowmarijuana.com/wp-content/uploads/2014/11/Ebb-and-Flow-Hydroponics-Diagram.jpg>
10. (n.d.). Retrieved May 19, 2015, from <http://www.simplyhydro.com/images/content/nft.gif>
11. (n.d.). Retrieved May 19, 2015, from http://howtogrowmarijuana.com/wp-content/uploads/2014/02/002_aerponics_system_diagram.png
12. Schubert, D., Quantius, D., Hauslage, J., Glasgow, L., Schroder, F., & Dorn, M. (2011). Advanced Greenhouse Modules for use within Planetary Habitats. 41st International Conference on Environmental Systems. Retrieved May 19, 2015, from <http://arc.aiaa.org/doi/pdf/10.2514/6.2011-5166>
13. Monje, O., Stutte, G., Goins, G., Porterfield, D., & Bingham, G. (2002). Farming in space: Environmental and biophysical concerns. *Advances in Space Research*, 151-167. Retrieved May

- 19, 2015, from http://ac.els-cdn.com/S0273117702007512/1-s2.0-S0273117702007512-main.pdf?_tid=1ec42206-fe56-11e4-b522-00000aab0f27&acdnat=1432060836_c0237175a6e30f3df6f2cc6103f02b40
14. Herridge, L. (2014, May 16). Veggie Plant Growth System Activated on International Space Station. Retrieved May 19, 2015, from <https://www.nasa.gov/content/veggie-plant-growth-system-activated-on-international-space-station>
 15. Hanger, B. (1993, May 1). Hydroponics in Antarctica. Retrieved May 19, 2015, from <http://www.hydroponics.com.au/issue-10-hydroponics-in-antarctica/>
 16. What is Photosynthetically Active Radiation? (2010, August 12). Retrieved May 19, 2015, from <http://www.fondriest.com/news/photosyntheticradiation.htm>
 17. Comstock, O. (2014, November 4). LED light bulbs keep improving in efficiency and quality. Retrieved May 19, 2015, from <http://www.eia.gov/todayinenergy/detail.cfm?id=18671>
 18. Campiotti, C., Alonzo, G., Belmonte, A., Bibbiani, C., Di Carlo, F., Dondi, F., & Scoccianti, M. (2009). Renewable Energy and Innovation for Sustainable Greenhouse Districts. Fascicula De Energetica, 15. Retrieved May 19, 2015, from <http://www.energy-cie.ro/archives/2009/p2-8.pdf>
 19. Martins, J. (2015). Smart Agricultural Façades; Cities' Greenest Energy Source.
 20. Tortorello, M. (2011, August 3). Finding the Potential in Vacant Lots. Retrieved May 19, 2015, from http://www.nytimes.com/2011/08/04/garden/finding-the-potential-in-vacant-lots-in-the-garden.html?_r=1
 21. Kaufman, J., & Bailkey, M. (2000). Farming Inside Cities: Entrepreneurial Urban Agriculture in the United States. Retrieved May 19, 2015, from <http://www.urbantilth.org/wp-content/uploads/2008/10/farminginsidocities.pdf>
 22. Culzac, N. (2014, July 12). Japanese plant experts produce 10,000 lettuce heads a day in LED-lit indoor farm. Retrieved May 19, 2015, from <http://www.independent.co.uk/news/science/japanese-plant-experts-produce-10000-lettuces-a-day-in-ledlit-indoor-farm-9601844.html>
 23. Seneviratne, K. (2012, December 12). Farming in the Sky in Singapore. Retrieved May 19, 2015, from <http://ourworld.unu.edu/en/farming-in-the-sky-in-singapore>
 24. Meinhold, B. (2013, May 27). FarmedHere: The Nation's Largest Indoor Organic Farm Now Growing in Chicago. Retrieved May 19, 2015, from <http://inhabitat.com/farmedhere-the-nations-largest-indoor-organic-farm-now-growing-in-chicago/>
 25. Vertical Farming Taking Root in Pennsylvania. (2014, July 24). Retrieved May 19, 2015, from <http://www.publicnewsservice.org/2014-07-24/rural-farming/vertical-farming-taking-root-in-pennsylvania/a40740-1>
 26. Peters, A. (2015, February 23). A Vacant Lot In Wyoming Will Become One Of The World's First Vertical Farms. Retrieved May 19, 2015, from <http://www.fastcoexist.com/3042610/a->

vacant-lot-in-wyoming-will-become-one-of-the-worlds-first-vertical-farms

27. Downtown Vancouver's rooftop garden closes, files for bankruptcy. (2014, January 25). Retrieved May 19, 2015, from <http://www.vancitybuzz.com/2014/01/downtown-vancouver-rooftop-garden-closes-files-bankruptcy/>
28. He, J., Tan, L., & Lee, S. (2009). Root-zone temperature effects on photosynthesis, 14C-photoassimilate partitioning and growth of temperate lettuce (*Lactuca sativa* cv. 'Panama') in the tropics. *Photosynthetica*, 47(1), 95-103. Retrieved May 19, 2015, from [http://download-v2.springer.com/static/pdf/350/art%3A10.1007%2Fs11099-009-0015-6.pdf?token2=exp=1432063563~acl=/static/pdf/350/art%253A10.1007%252Fs11099-009-0015-6.pdf*~hmac=c2925e5c090ac8bb757f19ace6b95125f035da6806a5d595c73773208fad35d0](http://download.v2.springer.com/static/pdf/350/art%3A10.1007%2Fs11099-009-0015-6.pdf?token2=exp=1432063563~acl=/static/pdf/350/art%253A10.1007%252Fs11099-009-0015-6.pdf*~hmac=c2925e5c090ac8bb757f19ace6b95125f035da6806a5d595c73773208fad35d0)
29. Hinman, T. (2011). Specialty Crops for Cold Climates. Retrieved May 19, 2015, from <http://www.aeromt.org/wordpress/wp-content/uploads/2012/05/Specialty-crops-for-cold-climates.pdf>
30. Morgan, L. (n.d.). Nutrient Temperature - Oxygen and Pythium in Hydroponics. Retrieved May 19, 2015, from http://www.simplyhydro.com/nutrient_temp.htm
31. Oxygenation, Air Pumps, Nutrient Uptake and Temperatures. (n.d.). Retrieved May 19, 2015, from http://www.quickgrow.com/gardening_articles/oxygenation_airpumps.html
32. Dissolved Oxygen and Biochemical Oxygen Demand. (n.d.). Retrieved May 19, 2015, from <http://water.epa.gov/type/rsl/monitoring/vms52.cfm>
33. Thompson, H., Langhans, R., Both, A., & Albright, L. (1998). Shoot and Root Temperature Effects on Lettuce Growth in a Floating Hydroponic System. *Journal of the American Society for Horticultural Science*, 123(3), 361-364. Retrieved May 19, 2015, from <http://journal.ashspublications.org/content/123/3/361.full.pdf>
34. Chun, C., & Takakura, T. (1994). Rate of Root Respiration of Lettuce under Various Dissolved Oxygen Concentrations in Hydroponics. *Environ. Control in Bio.*, 32(2), 125-135. Retrieved from https://www.jstage.jst.go.jp/article/ecb1963/32/2/32_2_125/_pdf
35. Goto, E., Both, A., Albright, L., Langhans, R., & Leed, A. (1996). Effect of Dissolved Oxygen Concentration on Lettuce Growth in Floating Hydroponics. *Acta Hort.*, 440, 205-210. Retrieved May 19, 2015, from <http://www.ncbi.nlm.nih.gov/pubmed/11541573>
36. Tse, A., & Ruth, W. (2006, November 1). Chilling The Root Zone. Retrieved May 19, 2015, from <http://www.hydroponics.com.au/issue-91-chilling-the-root-zone/>
37. Cambridge, MA Electricity Statistics. (n.d.). Retrieved May 19, 2015, from <http://www.electricitylocal.com/states/massachusetts/cambridge/>
38. Solfjeld, I., & Johnsen, O. (2006). The influence of root-zone temperature on growth of *Betula pendula* Roth. *Trees*, 20(3), 320-328. Retrieved May 19, 2015, from

<http://link.springer.com/article/10.1007/s00468-005-0043-1>

39. (n.d.). Retrieved May 19, 2015, from
<http://www.ce.utexas.edu/prof/kinnas/319lab/Book/CH1/PROPS/GIFS/dynwat.gif>
40. Winterborne, J. (2005). Hydroponics: Indoor Horticulture. Pukka Press.

Appendix

Arduino Air Temperature Control Code:

```
//include libraries for sensors, LCD, and clock
#include <Wire.h>
#include <OneWire.h>
#include <LiquidCrystal.h>
#include "RTClib.h"
RTC_DS1307 rtc;

//DS18S20 Temperature chip i/o
OneWire ds(10); // on pin 10

LiquidCrystal lcd(12,11,8,6,3,2);

//component locations on relay module
#define FANS 7
#define HEATER 4
#define LIGHTS 5

//temperature set points
float Tday = 30;
float Tnight = 25;

float Tmeas; //sensor temp reading, deg C
float delta; //difference between set point and Tmeas

void setup(){
  Serial.begin(9600);

  lcd.begin(16,2);

  Wire.begin();

  rtc.begin();

  pinMode(FANS, OUTPUT);
  pinMode(HEATER, OUTPUT);
  pinMode(LIGHTS, OUTPUT);

  // fans, heaters, and lights start off
  digitalWrite(FANS,HIGH);
  digitalWrite(HEATER,HIGH);
  digitalWrite(LIGHTS,HIGH);

  if (! rtc.isrunning() ) {
    Serial.println("RTC is NOT running!");
    // following line sets the RTC to the date & time this sketch was
    compiled
    //rtc.adjust(DateTime(F(__DATE__), F(__TIME__)));
    // This line sets the RTC with an explicit date & time
    rtc.adjust(DateTime(2015, 3, 18, 11, 30, 0));
  }
}
```

```

}

//rtc.adjust(DateTime(F(__DATE__), F(__TIME__)));
  rtc.adjust(DateTime(2015, 3, 18, 11, 30, 0));
}

void loop(){

  //retrieve time
  DateTime now = rtc.now();
  Serial.print("Hour:");
  Serial.println(now.hour(), DEC);
  //Hour = int(now.hour());
  Serial.print("Minute:");
  Serial.println(now.minute(), DEC);
  int Hour = now.hour();
  //Hour = Hour2.toInt();
  //Serial.print(Hour);

  //retrieve air temperature
  Tmeas = ReadTempVal();
  Serial.print("T measured = ");
  Serial.println(Tmeas);

  lcd.setCursor(0,0);
  lcd.print("Time: ");
  lcd.print(now.hour());
  lcd.print(":");
  lcd.print(now.minute());
  lcd.setCursor(0,1);
  lcd.print("T = ");
  lcd.print(Tmeas);
  lcd.print("oC");

  //daytime conditions

  if
(Hour==6||Hour==7||Hour==8||Hour==9||Hour==10||Hour==11||Hour==12||Hour
r==13||Hour==14||Hour==15||Hour==16||Hour==17||Hour==18||Hour==19||Hour
r==20||Hour==21||Hour==22||Hour==23){

    Serial.println("Daytime Mode, Lights ON");
    digitalWrite(LIGHTS,LOW);
    delta = Tmeas-Tday;
    delta_fun();
  }

  //nighttime conditions

  if (Hour==0||Hour==1||Hour==2||Hour==3||Hour==4||Hour==5){

```

```

    Serial.println("Nighttime Mode, Lights OFF");
    digitalWrite(LIGHTS,HIGH);
    delta = Tmeas-Tnight;
    delta_fun();
}
}

//Grove temperature probe setup
float ReadTempVal(){
    float TmeasFunc;
    int HighByte, LowByte, TReading, SignBit, Tc_100, Whole, Fract;
    byte i;
    byte present = 0;
    byte data[12];
    byte addr[8];

    if ( !ds.search(addr)) {
        ds.reset_search();

    }

    ds.reset();
    ds.select(addr);
    ds.write(0x44,1);// start conversion,w parasite power on at the end

    delay(1000);

    present = ds.reset();
    ds.select(addr);
    ds.write(0xBE); // Read Scratchpad

    for ( i = 0; i < 9; i++) { // we need 9 bytes
        data[i] = ds.read();
    }

    LowByte = data[0];
    HighByte = data[1];
    TReading = (HighByte << 8) + LowByte;
    SignBit = TReading & 0x8000; // test most sig bit

    if (SignBit){ // negative
        TReading = (TReading ^ 0xffff) + 1; }

    Tc_100 = (6 * TReading) + TReading / 4;

    Whole = Tc_100 / 100;
    Fract = Tc_100 % 100;

    float whole=float(Whole);
    float fract=float(Fract);

```

```

TmeasFunc=whole+fract/100;
return TmeasFunc;
}

void delta_fun(){
  if (delta < 0) {
    digitalWrite(FANS,HIGH);
    digitalWrite(HEATER, LOW);
    Serial.println("HEATER ON");
    Serial.println("FANS OFF");
    delay(20000);
  }

  else if (delta > 0) {
    digitalWrite(HEATER,HIGH);
    digitalWrite(FANS, LOW);
    Serial.println("FANS ON");
    Serial.println("HEATER OFF");
    delay(20000);
  }

  else {
    digitalWrite(HEATER,HIGH);
    digitalWrite(FANS,HIGH);
    Serial.println("ALL OFF");
    delay(20000);
  }
}
}

```

Arduino Water Temperature Control Code:

```
#include <OneWire.h>
#include <SoftwareSerial.h>

const int chipSelect = 4;

//DS18S20 Temperature chip i/o
OneWire ds(12); // on pin 11

//Initialize temperature vars
float Tmeas;
float Tset = 50; // define set point water temperature
float deltaT;
float Previous_deltaT;

//Declare delay between drive adjustments
float dt = 2000;

// Declare gains
float kP = 20;
float kI = 0;
float kD = 0;

//Initialize PID contributions
float P = 0;
float I = 0;
float WindupThresh = 5; //degrees C above which I term is zeroed
float D = 0;

//Set TEC driving parameters
float Duty = 0;
float Drive = 0;
float MapRange = 100;

#define rxPin 3 // pin 3 connects to smcSerial TX
#define txPin 4 // pin 4 connects to smcSerial RX

//Pololu relay setup
SoftwareSerial smcSerial = SoftwareSerial(rxPin, txPin);
// required to allow motors to move
// must be called when controller restarts and after any error

void exitSafeStart(){
```

```

smcSerial.write(0x83);}

// speed should be a number from -3200 to 3200
void setTECCapacity(int rate)

{
if (rate < 0){
smcSerial.write(0x86); // motor reverse command
rate = -rate; // make speed positive
}
else{
smcSerial.write(0x85); // motor forward command
}
smcSerial.write(rate & 0x1F);
smcSerial.write(rate >> 5);}

void setup(void) {
// initialize inputs/outputs

// start serial port

Serial.begin(9600;
smcSerial.begin(19200);
delay(5);
smcSerial.write(0xAA);
exitSafeStart();
}

//Grove temperature probe setup

float ReadTempVal(){
float TmeasFunc;
int HighByte, LowByte, TReading, SignBit, Tc_100, Whole, Fract;
byte i;
byte present = 0;
byte data[12];
byte addr[8];

if ( !ds.search(addr)) {
//Serial.print("No more addresses.\n");
ds.reset_search();
// TmeasFunc=0;
// return TmeasFunc;
}

// Serial.print("R=");
// for( i = 0; i < 8; i++) {
// Serial.print(addr[i], HEX);
// Serial.print(" ");
// }

```

```

    if ( OneWire::crc8( addr, 7) != addr[7]) {
        //Serial.print("CRC is not valid!\n");
//      TmeasFunc=0;
//      return TmeasFunc;
    }

    if ( addr[0] == 0x10) {
        //Serial.print("Device is a DS18S20 family device.\n");
    }

    else if ( addr[0] == 0x28) {
        //Serial.print("Device is a DS18B20 family device.\n");
    }
    else {
        //Serial.print("Device family is not recognized: 0x");
        //Serial.println(addr[0],HEX);
//      TmeasFunc=0;
//      return TmeasFunc;
    }

    ds.reset();
    ds.select(addr);
    ds.write(0x44,1);

    delay(1000);

    present = ds.reset();
    ds.select(addr);
    ds.write(0xBE);

//  Serial.print("P=");
//  Serial.print(present,HEX);
//  Serial.print(" ");
    for ( i = 0; i < 9; i++) {
        data[i] = ds.read();
//      Serial.print(data[i], HEX);
//      Serial.print(" ");
    }

//  Serial.print(" CRC=");
//  Serial.print( OneWire::crc8( data, 8), HEX);
//  Serial.println();
    LowByte = data[0];
    HighByte = data[1];
    TReading = (HighByte << 8) + LowByte;
    SignBit = TReading & 0x8000;
    if (SignBit) // negative
    {
        TReading = (TReading ^ 0xffff) + 1; // 2's com
    }

    Tc_100 = (6 * TReading) + TReading / 4;

    Whole = Tc_100 / 100; // separate off the whole and fractional
portions

```

```

Fract = Tc_100 % 100;
float whole=float(Whole);
float fract=float(Fract);
if (SignBit) // If its negative
{
    Serial.print("-");
}

//Serial.println(Whole);
//Serial.print(".");
// if (Fract < 10)
// {
//     Serial.print("0");
// }
//Serial.println(Fract);

Serial.print("\n");
TmeasFunc=whole+fract/100;
// Serial.print("Tmeas ");
// Serial.println(TmeasFunc);
return TmeasFunc;
//return;
}

void loop(void) {

Tmeas = ReadTempVal();
Serial.print("Tmeas ");
Serial.println(Tmeas);
deltaT = Tmeas-Tset;
Previous_deltaT = deltaT;

if (deltaT == 0) {
setTECcapacity(0);
    delay(dt);

Serial.print("Temperature at Tset, TEC running at duty 0");
}

else {
Serial.print("Temperature adjustment necessary. ");
P = deltaT;
    if (abs(deltaT) < WindupThresh) {
        I = I + deltaT*dt;
    }

    else {
        I = 0;
    }
}
}

```

```

D = (deltaT - Previous_deltaT)/dt;

Drive = P*kP + I*kI + D*kD;

Duty = map(Drive, -MapRange, MapRange, -3200, 3200);

  if (abs(Duty) <= 3200)    {
    setTECcapacity(Duty);
    delay(dt);
    Serial.print("TEC ran at duty ");
    Serial.println(Duty);
    Previous_deltaT = deltaT;
  }

  else {
    if (Duty<0){
      setTECcapacity(-3200);
      delay(dt);
      Serial.println("Potential Error: Drive out of mapping range,
        TEC ran at full reverse duty");

      Previous_deltaT = deltaT;
    }

    else {
      setTECcapacity(3200);
      digitalWrite(PUMP, LOW);
      delay(dt);
      Serial.println("Potential Error: Drive out of mapping range,
        TEC ran at full forward duty");
      Previous_deltaT = deltaT;
    }
  }
}
}
}
}

```

Processing Applet Code:

```
PImage bg;
int width;
int height;
PFont f;

import controlP5.*;
ControlP5 cp5;
DropDownList dl;

String TambDay = "?";
String TambNight = "?";
String TairDay = "?";
String TairNight = "?";
String TwaterDay = "?";
String TwaterNight = "?";
String DayHours = "?";
String NightHours = "?";
String GrowthDur = "?";
int NightHoursnum = 0;
String Thick = "?";
String SurfArea = "?";
String MassW = "?";
String PowAirDay = "=";
String PowWDay = "=";
String PowAirNight = "=";
String PowWNight = "=";
String kWh = "=";
String Dol = "=";

boolean TambDayready = false;
boolean TambNightready = false;
boolean TairDayready = false;
boolean TairNightready = false;
boolean TwaterDayready = false;
boolean TwaterNightready = false;
boolean DayHoursready = false;
boolean GrowthDurready = false;
boolean Thickready = false;
boolean SurfAreaready = false;
boolean MassWready = false;

float Kupper = 0;
float Rupper = 0;
float Tau = 33333; //sec
float Rlower = 0;
float McpH2O = 4187; //J/kgK
float Ecost = 14.91; //cents

float val = 0;
```

```

void setup() {
    // setup is called once at start up.
    width = 1004;
    height = 813;
    size(width, height);
    bg = loadImage("applet black white.png");
    f = createFont("Courier",24,true);

    cp5 = new ControlP5(this);
    cp5.setControlFont(new ControlFont(createFont("Courier", 18),
18));

    // create a DropDownList
    dl = cp5.addDropDownList("myList-dl")
        .setPosition(311, 560);

    customize(dl); // customize the first list
};

void customize(DropDownList ddl) {
    // a convenient function to customize a DropDownList

    ddl.setSize(190,100);
    ddl.setBackgroundColor(color(0));
    ddl.setItemHeight(20);
    ddl.setBarHeight(25);
    ddl.captionLabel().set("Jacket Material");
    ddl.captionLabel().style().marginTop = 3;
    ddl.captionLabel().style().marginLeft = 3;
    ddl.valueLabel().style().marginTop = 3;

    ddl.addItem("acrylic", 0);
    ddl.addItem("reflectix", 1);
    ddl.addItem("styrofoam", 2);
    ddl.addItem("wood", 3);

    //ddl.scroll(0);
    ddl.setColorBackground(color(0));
    ddl.setColorActive(color(255, 128));
}

void controlEvent(ControlEvent theEvent) {
    // DropDownList is of type ControlGroup.

    // A controlEvent will be triggered from inside the ControlGroup
class.

```

```

// therefore you need to check the originator of the Event with
// if (theEvent.isGroup())
// to avoid an error message thrown by controlP5.

if (theEvent.isGroup()) {
    // check if the Event was triggered from a ControlGroup
    println("event from group : "+theEvent.getGroup().getValue()+"
from "+theEvent.getGroup());

    val = theEvent.getGroup().getValue();
    println(val);
    if (val == 0.0){
        Kupper = 0.2;
    }

    else if (val == 1.0){
        Kupper = 0.02644;
    }

    else if (val == 2.0){
        Kupper = 0.033;
    }

    else if (val == 3.0){
        Kupper = 0.05;
    }
}

else if (theEvent.isController()) {
    println("event from controller :
"+theEvent.getController().getValue()+" from
"+theEvent.getController());
}
}

void draw(){
    // draw is called repeatedly
    // clear out the background

    background(bg);
    textFont(f,24);

    text(TambDay,375,207);
    text(DayHours,333,56);
    fill(255,255,255);

    text(TambNight,875,208);
    text(TairDay,234,271);
}

```

```

text(TairNight,733,272);
text(TwaterDay, 234,460);
text(TwaterNight,733,461);
text(NightHours,832,56);
text(GrowthDur,335,792);
text(Thick,438,582);
text(SurfArea,438,610);
text(MassW,796,549);
fill (0,0,0);

Rupper = float(Thick)/100/Kupper/float(SurfArea);
Rlower = Tau/McpH2O/float(MassW);

float PowAirDay = abs((float(TambDay)-float(TairDay))/Rupper);
float PowAirNight = abs((float(TambNight)-
float(TairNight))/Rupper);

float PowWDay = abs((float(TairDay)-float(TwaterDay))/Rlower);
float PowWNight = abs((float(TairNight)-
float(TwaterNight))/Rlower);

float AvgW =
(float(DayHours)*(PowAirDay+PowWDay)+float(NightHours)*(PowAirNight+Po
wWNight))/24;

float kJ = float(GrowthDur)*24*360*AvgW/1000;
float kWh = kJ/3600;
String.format("%.1f", kWh);
float Dol = Ecost*kWh/100;
String.format("%.2f", Dol);

text(round(PowAirDay),83,698);
text(round(PowWDay),322,698);
fill(255,255,255);
text(round(PowAirNight),575,698);
text(round(PowWNight),813,698);
text(kWh,628,790);
text(Dol,897,790);
fill (0,0,0);

};

//void entervalue(String temp, boolean overtemp, boolean tempready){
void mousePressed(){
    if (mouseX > 373 && mouseX < 428 &&
        mouseY > 188 && mouseY < 211){
        println("TambDay");
        TambDayready = true;
        TambNightready = false;
        TairDayready = false;

```

```

    TwaterDayready = false;
    TwaterNightready = false;
    DayHoursready = false;
    GrowthDurready = false;
    Thickready = false;
    SurfAreaready = false;
}

else if (mouseX > 873 && mouseX < 926 &&
        mouseY > 187 && mouseY < 212){
    println("TambNight");
    TambNightready = true;
    TambDayready = false;
    TairDayready = false;
    TairNightready = false;
    TwaterDayready = false;
    TwaterNightready = false;
    DayHoursready = false;
    GrowthDurready = false;
    Thickready = false;
    SurfAreaready = false;
    MassWready = false;
}

else if (mouseX > 232 && mouseX < 286 &&
        mouseY > 252 && mouseY < 275){
    println("TairDay");
    TairDayready = true;
    TambDayready = false;
    TambNightready = false;
    TairNightready = false;
    TwaterDayready = false;
    TwaterNightready = false;
    DayHoursready = false;
    GrowthDurready = false;
    Thickready = false;
    SurfAreaready = false;
    MassWready = false;
}

else if (mouseX > 731 && mouseX < 783 &&
        mouseY > 252 && mouseY < 276){
    println("TairNight");
    TairNightready = true;
    TambDayready = false;
    TambNightready = false;
    TairDayready = false;
}

```

```

    TwaterDayready = false;
    TwaterNightready = false;
    DayHoursready = false;
    GrowthDurready = false;
    Thickready = false;
    SurfAreaready = false;
    MassWready = false;
}

else if (mouseX > 232 && mouseX < 287 &&
        mouseY > 441 && mouseY < 464){
    println("TwaterDay");
    TwaterDayready = true;
    TambDayready = false;
    TambNightready = false;
    TairDayready = false;
    TairNightready = false;
    TwaterNightready = false;
    DayHoursready = false;
    GrowthDurready = false;
    Thickready = false;
    SurfAreaready = false;
    MassWready = false;
}

else if (mouseX > 731 && mouseX < 784 &&
        mouseY > 441 && mouseY < 465){
    println("TwaterNight");
    TwaterNightready = true;
    TambDayready = false;
    TambNightready = false;
    TairDayready = false;
    TairNightready = false;
    TwaterDayready = false;
    DayHoursready = false;
    GrowthDurready = false;
    Thickready = false;
    SurfAreaready = false;
    MassWready = false;
}

else if (mouseX > 331 && mouseX < 365 &&
        mouseY > 36 && mouseY < 61){
    println("DayHours");
    DayHoursready = true;
    TambDayready = false;
    TambNightready = false;
    TairDayready = false;
    TairNightready = false;
    TwaterDayready = false;

```

```

    TwaterNightready = false;
    GrowthDurready = false;
    Thickready = false;
    SurfAreaready = false;
    MassWready = false;
}
else if (mouseX > 333 && mouseX < 402 &&
        mouseY > 773 && mouseY < 796){
    println("GrowthDur");
    GrowthDurready = true;
    TambDayready = false;
    TambNightready = false;
    TairDayready = false;
    TairNightready = false;
    TwaterDayready = false;
    TwaterNightready = false;
    DayHoursready = false;
    Thickready = false;
    SurfAreaready = false;
    MassWready = false;
}
else if (mouseX > 436 && mouseX < 500 &&
        mouseY > 562 && mouseY < 586){
    println("Thick");
    Thickready = true;
    TambDayready = false;
    TambNightready = false;
    TairDayready = false;
    TairNightready = false;
    TwaterDayready = false;
    TwaterNightready = false;
    DayHoursready = false;
    GrowthDurready = false;
    SurfAreaready = false;
    MassWready = false;
}
else if (mouseX > 436 && mouseX < 500 &&
        mouseY > 590 && mouseY < 614){
    println("SurfArea");
    SurfAreaready = true;
    TambDayready = false;
    TambNightready = false;
    TairDayready = false;
    TairNightready = false;
    TwaterDayready = false;
    TwaterNightready = false;
    DayHoursready = false;
}

```

```

    GrowthDurready = false;
    Thickready = false;
    MassWready = false;
}
else if (mouseX > 794 && mouseX < 857 &&
        mouseY > 529 && mouseY < 553){
    println("MassW");
    MassWready = true;
    TambDayready = false;
    TambNightready = false;
    TairDayready = false;
    TairNightready = false;
    TwaterDayready = false;
    TwaterNightready = false;
    DayHoursready = false;
    GrowthDurready = false;
    Thickready = false;
    SurfAreaready = false;
}
};

void keyPressed() {
    if (TambDayready){
        if (keyCode == BACKSPACE) {
            if (TambDay.length() > 0) {
                TambDay = TambDay.substring(0, TambDay.length()-1);
            }
        }
        else if (keyCode == DELETE) {
            TambDay = "";
        } else if (keyCode != SHIFT && keyCode != CONTROL && keyCode != ALT)
        {
            TambDay = TambDay + key;
        }
    }
}
else if (TambNightready){
    if (keyCode == BACKSPACE) {
        if (TambNight.length() > 0) {
            TambNight = TambNight.substring(0, TambNight.length()-1);
        }
    } else if (keyCode == DELETE) {
        TambNight = "";
    } else if (keyCode != SHIFT && keyCode != CONTROL && keyCode != ALT)
    {
        TambNight = TambNight + key;
    }
}

```

```

    }
}
else if (TairDayready){
if (keyCode == BACKSPACE) {
    if (TairDay.length() > 0) {
        TairDay = TairDay.substring(0, TairDay.length()-1);
    }
} else if (keyCode == DELETE) {
    TairDay = "";
} else if (keyCode != SHIFT && keyCode != CONTROL && keyCode != ALT)
{
    TairDay = TairDay + key;
}
}
else if (TairNightready){
    if (keyCode == BACKSPACE) {
        if (TairNight.length() > 0) {
            TairNight = TairNight.substring(0, TairNight.length()-1);
        }
    } else if (keyCode == DELETE) {
        TairNight = "";
    } else if (keyCode != SHIFT && keyCode != CONTROL && keyCode != ALT)
    TairNight = TairNight + key;
}
}
else if (TwaterDayready){
    if (keyCode == BACKSPACE) {
        if (TwaterDay.length() > 0) {
            TwaterDay = TwaterDay.substring(0, TwaterDay.length()-1);
        }
    } else if (keyCode == DELETE) {
        TwaterDay = "";
    } else if (keyCode != SHIFT && keyCode != CONTROL && keyCode != ALT)
    {
        TwaterDay = TwaterDay + key;
    }
}
else if (TwaterNightready){
    if (keyCode == BACKSPACE) {
        if (TwaterNight.length() > 0) {
            TwaterNight = TwaterNight.substring(0, TwaterNight.length()-1);
        }
    }
}

```

```

    } else if (keyCode == DELETE) {
        TwaterNight = "";
    } else if (keyCode != SHIFT && keyCode != CONTROL && keyCode != ALT)
    {
        TwaterNight = TwaterNight + key;
    }
}

else if (DayHoursready){
    if (keyCode == BACKSPACE) {
        if (DayHours.length() > 0) {
            DayHours = DayHours.substring(0, DayHours.length()-1);
        }

        } else if (keyCode == DELETE) {
            DayHours = "";
        } else if (keyCode != SHIFT && keyCode != CONTROL && keyCode != ALT)
DayHours = DayHours + key;
    }

    NightHoursnum = 24-int(DayHours);
    NightHours = Integer.toString(NightHoursnum);
}

else if (GrowthDurready){
    if (keyCode == BACKSPACE) {
        if (GrowthDur.length() > 0) {
            GrowthDur = GrowthDur.substring(0, GrowthDur.length()-1);
        }

        } else if (keyCode == DELETE) {
            GrowthDur = "";
        } else if (keyCode != SHIFT && keyCode != CONTROL && keyCode != ALT)
    {
        GrowthDur = GrowthDur + key;
    }
}

else if (Thickready){
    if (keyCode == BACKSPACE) {
        if (Thick.length() > 0) {
            Thick = Thick.substring(0, Thick.length()-1);
        }

        } else if (keyCode == DELETE) {
            Thick = "";
        } else if (keyCode != SHIFT && keyCode != CONTROL && keyCode != ALT)
    {
        Thick = Thick + key;
    }
}
}

```

```

else if (SurfAreaready){
  if (keyCode == BACKSPACE) {
    if (SurfArea.length() > 0) {
      SurfArea = SurfArea.substring(0, SurfArea.length()-1);
    }

    } else if (keyCode == DELETE) {
      SurfArea = "";
    } else if (keyCode != SHIFT && keyCode != CONTROL && keyCode != ALT)
{
  SurfArea = SurfArea + key;
}
}

else if (MassWready){
  if (keyCode == BACKSPACE) {
    if (MassW.length() > 0) {
      MassW = MassW.substring(0, MassW.length()-1);
    }
    } else if (keyCode == DELETE) {
      MassW = "";
    } else if (keyCode != SHIFT && keyCode != CONTROL && keyCode != ALT)
{
  MassW = MassW + key;
}
}
};

```